ADDIS ABABA UNIVERSITY

ADDIS ABABA INSTITUTE OF TECHNOLOGY

SCHOOL OF ELECTRICAL AND COMPUTER ENGINEERING

Performance Analysis of Downlink Linear Precoding for Multi-Cell Massive MIMO under Correlated Rayleigh Fading Channels

---

By:

Habte Aregawi

Advisor:

Dr. Murad Ridwan

A thesis submitted in partial fulfillment of the requirements for the degree of Masters of Science in Communication Engineering.

November 2022
Addiss Ababa, Ethiopia

ADDIS ABABA UNIVERSITY

ADDIS ABABA INSTITUTE OF TECHNOLOGY

SCHOOL OF ELECTRICAL AND COMPUTER ENGINEERING

The signatories have examined the thesis titled:

Performance Analysis of Downlink Linear Precoding for Multi-Cell Massive MIMO under Correlated Rayleigh Fading Channels

Habte Aregawi, a candidate for the Master of Science degree, has presented it and certifies that it is worthy of acceptance.

Approval by Boards of Examiners

Chairman, Dept. Graduate Committee	Date	Signature
Dr. Murad Redwan Advisor	Date	Signature
Internal Examiner	Date	Signature
External Examiner	Date	Signature

Declaration

I hereby certify that this report constitutes my own product, that where the language of others is set forth, quotation marks so indicate, and that appropriate credit is given where I have used the language, ideas, expressions or writings of another.

I declare that the report describes original work that has not previously been presented for the award of any other degree of any institution.

Habte Aregawi	_____	_____
Name	signature	Date of submission

Place: Addis Ababa, Ethiopia

Acknowledgement

To begin, I would like to thank my supervisor, Dr. Murad, for his unwavering support throughout my thesis work and for devoting his valuable time to encouraging me to work in my own way and giving me the freedom to delve deeply into this study; without his excellent assistance, I would not have been able to achieve the study's ultimate goal. He was always willing to help me when I had an issue with my thesis.

Mr. Siefu Girma (PhD. Cand.) deserves special thanks for his patient direction, encouragement, and invaluable oversight throughout the research.

Mr. Samuel Tekele, my brother, is also to be thanked. The numerous times you aided me in every element of my life along my trip is unimaginable.

It is simply impossible to list the names of a significant number of friends and well-wishers who gave individual assistance, either directly or indirectly, in carrying out this initiative in this restricted area. I owe a huge debt of gratitude to everyone who helped me get where I needed to go.

Abstract

The Fifth Generation (5G) networks have performance targets of high Spectral Efficiency (SE), decreased latency, energy savings, cost reduction, high system capacity, and huge device connections. To increase the SE of networks, researchers deal with increasing the transmit power, obtaining the array gain, using Space Division Multiple Access (SDMA), and deploying massive numbers of antennas at the Base Station (BS). A Multi User-Multiple Input Multiple Output (MU-MIMO) technology that combines SDMA with Time Division Duplex (TDD) to limit the Channel State Information (CSI) acquisition overhead and a massive number of antennas at the BS is known as Massive-Multiple Input Multiple Output (M-MIMO). For efficient use of massive antennas at the BS, the channel characteristics between User Equipments (UEs) and the BS must be known. Practical channels are known to be spatially correlated due to sampling at the BS, environmental orientations, and polarization effects. Estimation of spatially correlated channels in a multi-cell M-MIMO system degrades due to reuse of pilot signals among UEs, which cannot be addressed by increasing the number of BS antennas.

Alleviating the impact of pilot contamination in multi-cell cellular systems is conducted in various research. However, describing pilot contamination effects based on UEs position on the channel estimation is not addressed in most of the researches.

In this research, the effect of UEs position on channel estimation and the ability to get favourable channels is investigated under correlated Rayleigh fading channels. Using blind estimation of precoded channels, the performance of different linear precoding schemes is examined using MATLAB simulation platform.

The pilot contamination effect is negligible under more correlated channels if the angle of arrival (position of UEs) is slightly different. The Minimum Mean Square Error (MMSE) precoding schemes have better performance than Regularized Zero Forcing (RZF), Zero Forcing (ZF), and Maximum Ratio Transmission (MRT). RZF has better performance than ZF when the effective Signal to Noise Ratio (SNR) is low or the number of antennas at the BS is small, unless they have the same level of performance.

Keywords: Spectral Efficiency, Massive MIMO, Pilot Contamination, Linear Precoding, MMSE, RZF, ZF, MRT .

Contents

List of Figures

List of Tables

Acronym

3D	Three Dimensions
3GPP	3rd Generation Partnership Project
5G	Fifth Generation
ASD	Angular Standard Deviation
AoA	Angle of Arrival
BS	Base Station
CSI	Channel State Information
CSIT	Channel State Information at Transmitter
DL	DownLink
DPC	Dirty Paper Coding
EM	Electro-magenetic
EMBB	Enhanced Mobile Broadband
I.I.D	Independently and Identically Distributed
mmWave	Millmeter Wave
MIMO	Multiple Input Multiple Output
M-MIMO	Massive-Multiple Input Multiple Output
MMSE	Minimum Mean Square Error
MMTC	massive Machine Type Communication
MRT	Maximum Ratio Transmission
MSE	Mean Square Error
MU-MIMO	Multi User-Multiple Input Multiple Output
NLoS	Non Line of Sight
NMSE	Normalized Mean Square Error
PDF	Probability Density Function
RZF	Regularized Zero Forcing
SDMA	Space Division Multiple Access
SINR	Signal to Interference plus Noise Ratio
SNR	Signal to Noise Ratio
SE	Spectral Efficiency
TDD	Time Division Duplex
THP	Tomlinson-Harashima Precoding
UEs	User Equipments
UE	User Equipment
UHD	Ultrahigh Definition
URLLC	Ultra-Reliable and Low Latency Communications
UL	UpLink
ULA	Uniform Linear Array
ZF	Zero Forcing

List of Symbols

τ_c	*Coherence time interval*
h	*Scalar h*
$\mathbf{h}$	*Vector h*
H	*Matrix H*
$\mathbb{R}$	*Set of real numbers*
$\mathbb{C}$	*Set of complex numbers*
$(.)^*$	*Complex conjugate*
$(.)^T$	*Transpose of matrix*
$(.)^H$	*Hermitian of matrix*
$tr(.)$	*Trace of square matrix*
$(.)^{-1}$	*Inverse of matrix*
I_N	*Identity matrix with size N*
$\mathbb{E}\{.\}$	*Mean of the random variable*
$\|.\|$	*Norm of vector*
$\|.\|$	*Absolute value*
$\mathcal{CN}(0,\sigma^2)$	*Circularly symmetric complex Gaussian random variable with variance* σ^2
$\mathcal{N}(0,\sigma^2)$	*Gaussian random variable with zero mean and variance* σ^2

Chapter 1

Background and Motivation

1.1 Introduction

High SE, decreased latency, energy savings, cost reduction, high system capacity, and huge device connection are all performance goals for the 5G of mobile cellular communication [1]. Enhanced Mobile Broadband (EMBB), massive Machine Type Communication (MMTC), and Ultra-Reliable and Low Latency Communications (URLLC) are the three use cases for 5G networks, as indicated in Figure 1.1 [2]

EMBB covers human-centric use cases for accessing multimedia content, services, and data (for example: Three Dimensions (3D) films, Ultrahigh Definition (UHD) displays, augmented reality, and so on). URLLC has strict standards for throughput, latency, and availability (e.g., industry automation, mission-critical applications, self-driving cars, etc.). MMTC is used in cases where many linked devices are communicating a small amount of non-delay sensitive data (e.g., smart grids, smart homes/buildings, smart cities, etc.) [2].

From the listed performance targets in [1], SE is an encoded or decoded scheme that determines how many information bits per complex-valued sample we can transmit reliably under channel consideration. If we consider a fading channel that changes at a time, the SE can be viewed as the average number of $bits/s/Hz$ under fading realizations. To increase the SE the researcher deals with increasing the transmit power, increasing cell density, acquiring CSI, and increasing the number of antennas.

Multiple Input Multiple Output (MIMO) technologies have received considerable attention for modern wireless communication systems because they can substantially increase the performance targets mentioned [1]. A MU-MIMO technology called M-MIMO which have M active antenna elements at the BS and utilizes this to communicate with single antenna K terminals over the same time and frequency resources gain a wide attention from academia and industry [3, 4]. The number of antennas at the base station exceeds the number of UEs components in the cell ($^{M}/_{K} \geq 1$). Using massive number of antenna arrays we can achieve favorable channels (channels with orthogonal Eigen spaces) at BS [3, 5]. Array gain and multiplexing gain are used to achieve high throughput and energy efficiency [6–8]. M-MIMO distinguished from traditional MU-MIMO in three ways; CSI is performed at the BS only, the total number of UEs is less than the total number of BS antennas, and basic linear signal processing is utilized on both the UpLink (UL)

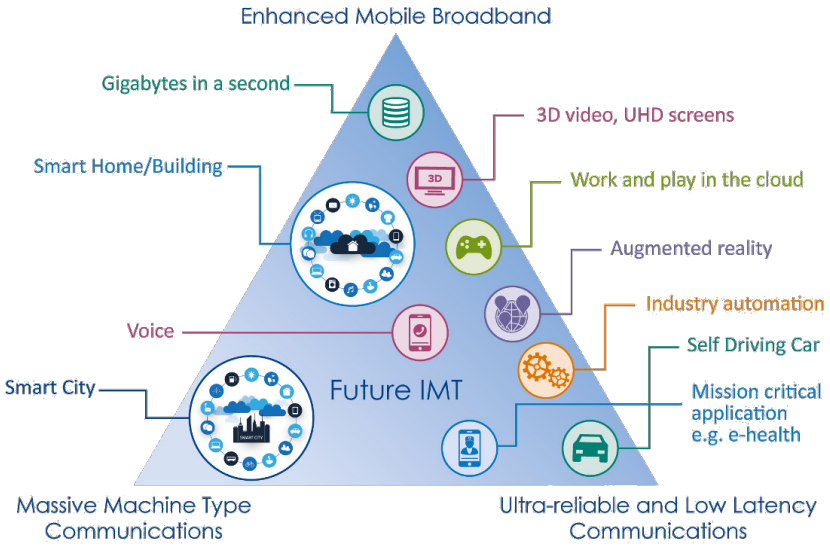

Figure 1.1: 5G Use Case [2]

and DownLink (DL) [9, 10].

In M-MIMO, the BS estimates the channel characteristics of UEs from UL pilots signals. In TDD operation the channels are reciprocal, the estimation in the UL is directly used in the DL under consideration of some constraints. From practical observations faded channels are found to be spatially correlated due to; more multipath being produced in some direction because of propagation environment, the geometry of the array produces spatially over and under-sampling, and spatial dependency of antenna pattern and varying polarization of the transmitted signal [11, 12]. Terminal mobility limits TDD M-MIMO operation, resulting in a short coherence block and a restricted number of orthogonal pilots. In a multi-cell system, the home cell's pilots are reused in neighboring cells to a degree known as the pilot reuse factor r, contaminating channel estimates results in the home cell with those of other cells utilizing the same pilots. This is known as pilot contamination [13, 14], and it causes channel estimation to degrade as well as interference from the same pilot UEs, which cannot be addressed by increasing the number of BS antennas.

In this research, the channel model $\mathbf{h}$ considers that the BS equipped with a uniform linear array have an elevation that will not produce scattering in its near-field, so that, the scattering is localized around the UEs only.

A flexible approach for delivering signals from an array of M antennas to one or more UEs is transmit precoding. DL precoding is a strategy that takes use of broadcast diversity by weighting the data stream, i.e., the transmitter delivers the coded data to the recipient to achieve channel pre-information. In different precoding techniques, the linear precoding techniques that consider blind estimation of precoded channel in the downlink such as minimum mean square error MMSE, RZF, ZF, and MRT are considered based on principle of UL-DL duality vector design method in this research.

1.2 Problem Statement

SE, link reliability, coverage, and energy efficiency are all key difficulties in 5G cellular network communication. The difficulties are caused by the limited available bandwidth, the fading nature of the propagation channel, and the mobility of the wireless nodes. To minimize SE degradation, researchers have been focusing on using M-MIMO and conventional signal processing techniques in line with the channel conditions between the source and destination. Practical wireless channels are found to be spatially correlated, where the gain and the direction of the fading channel are correlated.

The mobility of terminals limits M-MIMO operation, resulting in a brief coherence block and a restricted number of orthogonal pilots. In a multi-cell system, the home cell's pilots are reused in nearby cells, contaminating channel estimation results in the home cell by neighboring cells employing the same pilot signals. This causes channel estimation to degrade, as well as interference from the same pilot UEs during data transmission, which cannot be addressed by increasing the number of BS antennas.

This encourages us to continue working on the subject. The majority of the research was conducted on single-cell [15,16] and multi-cell link-level [3,17] performance studies of linear precoding in both correlated and uncorrelated fading channels. However, describing pilot contamination effects based on UEs position on the channel estimation is rarely reported. The effect of UEs (that share the same pilot sequence) position (azimuth angle) towards BS on channel estimation at the home cell under correlated fading channels needs to be explored. The impact of estimated channels on the SE in the DL using different linear precoding schemes also needs to be examined.

1.3 Related Work

In 2010, the author in [3] described the possibility of deploying massive antennas at the BS using uncorrelated fading channels. Generalize that, as the number of BS antennas grows without limit, all of the effects of uncorrelated noise and fast fading disappear. What remains is inter-cellular interference that results from pilot contamination.

In [15], in partial fulfillment of the requirements for the degree of master of science, observed the performance of linear precoding techniques for 5G massive MIMO with perfect and imperfect Channel State Information at Transmitter (CSIT). It is concluded that the performance of linear precoding is better when the transmitter has perfect CSI.

The combined work in [16], studied the performance of linear precoding in a single-cell scenario for very large MU-MIMO DL systems. Examinations consider MMSE, ZF, and MRT linear precoding schemes. The result shows that MMSE and ZF have the same performance when the number of antennas at the BS is beyond 25.

Enhancing the performance of cellular user SE under pilot contamination was studied in [17]. They modeled the random channel using Laplacian distributed scattering model. It is observed that spatial channel correlation increases the degree of favorable propagation when the UEs have different spatial characteristics. The highest SE of the proposed Laplacian centralized scattering spatially correlated Rayleigh fading model is achieved when using the MMSE precoding scheme with a pilot reuse factor of four.

Authors in [18], explored the requirement of a pilot signal for precoded channel estimation in DL transmission. The result implies, there is no need for pilot signaling in the DL to maximize the spectral efficiency. They showed that the precoded signal can be estimated in the DL by the UEs blindly, if the channel does not show channel hardening with a given number of antennas.

M-MIMO in multi-cell scenarios with highly complex signal processing known as MMSE scheme was investigated in [19]. Their proposed method achieved good sum SE in single-cell deployment scenario. For multi-cell M-MIMO deployment scenarios, research in [20] was conducted for uncorrelated fading channels in the UL transmission.

Researchers in [15, 16, 19] findings limited to single cell, where there will not be any pilot contamination in communication channel. Their channel modeling is also uncorrelated fading, as practical channel are practically correlated. Since the scenario is limited to uncorrelated fading and single-cell, the SE in the DL using MMSE and ZF precoding vector have the same value after limited number of antennas, which is not true in multi-cell and correlated fading channels.

Literature's in [3, 18, 20], deploy a multi-cell systems scenario that considers the pilot contamination effect, but the impact of spatial correlation on channel did not considered in their findings. Since the their channel model is uncorrelated fading, per antenna correlation coefficient is always unity regardless of the eigenstructure of the UEs. the channel The combined impact of pilot contamination and spatial correlation was investigated in [17], where the SE bound was considered the hardening bound. The number of antennas they deployed at the BS which is not practical.

1.4 Research Objective

General Objective

Performance Analysis of Downlink Linear Precoding for Multi-Cell Massive MIMO under Correlated Rayleigh Fading Channels.

Specific Objective

- Modeling of local scattering spatial correlation channel.
- Channel estimation at the base station.
- Spatial correlation fading channels effect on channel hardening and favorable propagation.
- Pilot contamination impact on channel estimation.
- Deriving closed-form lower bound spectral efficiency in the downlink.
- Selecting precoding vector design.
- Analyze linear precoding in the downlink.

1.5 Contributions of the Research

In all the literature's seen so far in Section 1.3, precoding has been investigated at various levels. However, some of the differences in the previous work and the current work are underlined in the following points.

- Characterizing pilot contamination effect based on UEs locations.
- The impact of the terminal position on the estimation of random channels.
- Advantage of using blind estimation for the precoded channel.
- Impact of channel correlation on the performance of the SE in the DL.
- SE for different precoding schemes using Monte Carlo simulation for random distribution of UEs.

1.6 Methodology

This research work will follow a quantitative research approach to make quantitative descriptions, measure, and compare linear precoding parameters. The data is collected from deep literature review on books, journals and other related works, to understand basic concepts behind the spatial correlated fading channels and linear precoding techniques. It also considered as a means of finding research gap and making a comparative study. The remaining paramount data is collected during parametric comparison of existing methods through simulation. Theoretical data analysis is based on information gathered from literature reviews and observations, and it can be stated as a comparison of various study findings.

Under correlated Rayleigh fading channel modeling, the impact of pilot contamination on channel estimation based on terminals distribution is investigated. Using different linear precoding schemes such as MMSE, RZF, ZF, and MRT are utilized to analyze the model's SE in the DL. The mathematical model and measurable parameters of the research are implemented using MATLAB simulation platform. Later on, the effect of spatial correlation on the performance of various linear precoding schemes is examined, compared and reported.

1.7 Thesis Outline

The research content is composed as the following scenarios:

- Chapter 2, introduce the theoretical and ways of improving SE, background of M-MIMO, background of channel estimation and DL linear precoding, and theory of channel hardening and favourable propagation.
- Chapter 3, local scattering channel modeling, pilot signalling for channel estimation in the UL using MMSE estimation technique, DL precoding vector such as MMSE, RZF, ZF, and MRT.
- Chapter 4, provides the simulation results and discussion of impact of spatial correlation on channel hardening, favourable propagation, estimation quality, and the SE in the DL using different precoding techniques.
- Chapter 5, presented the conclusion of the research and recommendation for future work.

Chapter 2

Spectral Efficiency

2.1 Introduction

SE is an encoded or decoded scheme that determines how much information bits per complex-valued sample, we can transmit reliably under channel consideration. The Nyquist-Shannon sampling theorem states that the band-limited communication signal passing through a channel with a bandwidth of B Hz is completely determined by $2B$ real-valued equal-spaced samples per second, B complex-valued samples per second are the more natural quantity when considering the complex-baseband representation of the signal. Thus, B complex-valued samples are the degrees of freedom available for designing the communication signal. We can see that the SE is a deterministic number that can be measured in bit per complex-valued sample. If we consider a fading channel that changes at a time, the SE can be viewed as the average number of bits/s/Hz under fading realizations.

In the consecutive portion of this chapter, we consider SE of the channel between BS and UEs refers to the SE of the UE. The information rate $[bit/s]$, which is a parallel measure, is calculated by dividing the SE by the bandwidth B. Additionally, the aggregate SE (measured in $bit/s/Hz/cell$) of the channels from all UEs in a cell to the associated BS, is often considered

2.2 Capacity of Communication Channel

Depending on how to select encoding or decoding schemes, The channel between terminals at given locations can support many different SEs, but in designing communication systems, how large the achievable SE is a key important point. Claude Shannon in 1948 was defined, channel capacity can determine the SE of a communication system [21].

Considering Figure 2.1, when the channel dispersion between samples is significantly less than the effective time interval, the channel becomes memory-less. With that, we can construct a discrete memory-less interference channel with input $x \in \mathbb{C}$ and output $y \in \mathbb{C}$ as follows:

$$y = hx + v + n \tag{2.1}$$

where $n \sim \mathcal{N}_C(0, \sigma^2)$ denotes independent noise, $h \in \mathbb{C}$ is the channel response at the

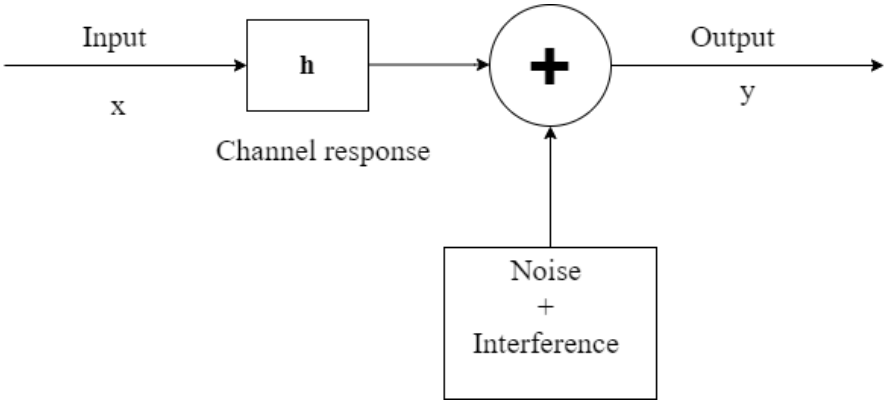

Figure 2.1: Communication Channel

output, and $v \in \mathbb{C}$ denotes random interference. The input is power-limited as $\mathbb{E}\left\{|x|^2\right\} \leq p$.

If u is a random variable with realization $\mathbb{U}$ that impacts the interference variance and h is a realization of the random variable $\mathbb{H}$. These random variables' realizations are known at the output. If the noise n is conditionally independent of given h and u, the interference v has conditional zero mean (i.e.,$\mathbb{E}\{v|h,u\} = 0$) and conditional variance denoted by $pv\,(h,v) = \mathbb{E}\{|v|^2\,|h,u\}$, and the interference is conditionally uncorrelated with the input (i.e.,$\mathbb{E}\{x^*v|h,u\} = 0$ then the ergodic channel capacity C is lower bounded as [22]:

$$C \geq \mathbb{E}\left\{\log_2\left(1 + \frac{p\,|h|^2}{pv\,(h,u) + \sigma^2}\right)\right\} \tag{2.2}$$

Where the bound is achieved using the input distribution $x \sim \mathcal{N}_C\,(0,p)$. Interference term treated as an additional source of noise in the decoder, to obtain the lower bound channel capacity. In the low-interference region, the lower bound capacity is optimal to treat interference as additional noise, as shown in [23–27]. In case of strong interference, the bound cannot be considered optimal in the information-theoretic view.

The SE expressions derived will be used throughout this document. We must know that the achievable SEs though not the best, SEs can be obtained via the receiver's low-complexity signal processing, which treats interference as noise.

From the expression, the Signal to Interference plus Noise Ratio (SINR) for considering h and pv are deterministic.

$$SINR = \frac{p\,|h|^2}{pv + \sigma^2} \tag{2.3}$$

2.3 Spectral Efficiency Improvement Techniques

Due to technological advancements, the demand for high data rate is also increasing. To alleviate limitation of resources, the researcher deals to the following ways of optimizing the SE. Here, we listed the way we can increase SE with its limitations.

Transmit Power: increasing the transmit power of UEs will increase the SNR and improves the SE, but no extraordinary SEs can be obtained when the network pushed into

an interference-limited regime. This effect is due to the BS have no degrees of freedom, which make it impossible to distinguish between intended signal and interference with only one observation.

Cell Density: Another way to increase the SE is increasing the cell density D, while the transmit power keep fixed. The average channel gain is typically assumed to be inversely related to propagation distance to some given path-loss exponent in channel modeling. In such a basic propagation model, when D is increased, the strength of the received desired signal and the inter-cell interference both rise at nearly the same rate, because both the distance to the desired BS and the distance to the interfering BSs are shortened. Although D cannot be significantly increase at coverage levels, cell densification is a convenient way to improve hotspot levels [28]. Area throughput increases linearly with D, if the basic propagation model is hold true. However, at some point this model will be disable. This is because the path loss index also decreases with distance, approaching a free space expansion scenario with an index of two [8]. In this extremely short-range scenario, cell compression is no longer desirable because the total power of the interfering signal increases faster than the desired signal power.

Array Gain: BS can use multiple receiving antennas to collect more energy from Electromagenetic (EM) waves instead of increasing UL transmit power. This concept has existed since at least the 1930s [29,30], with a particular focus on achieving spatial diversity. That is, multiple receiving antennas that monitor the realization of different fading's are used to counter channel fading during Non Line of Sight (NLoS) propagation. The related idea of using several transmitting antennas to increase the received signal power was explain as early as 1919 [31]. The presence of multiple receiving antennas also allows the receiver to use spatial filtering/processing to distinguish signals with different spatial directivity [32]. Implementations of these methods are called adaptive or intelligent antennas [33, 34]. It is more convenient to equipped the BS with many antennas than the UEs. This is due to UEs are compact commercial end-use products that typically run-on batteries and rely on inexpensive components. The scaling behavior obtained by the above asymptotic analysis was experimentally verified for the actual number of antennas [35,36]. However, it is important to note that the propagation environment is surrounded by the finite volume method, so physics cannot increase the size of an array indefinitely with $M \to \infty$ [37]. Ideally, you can cover the surface of this volume with an antenna and ignore the absorption to collect all the signal energy, but you cannot collect more energy than it was transmitted. When dealing with hundreds or thousands of antennas, a large channel gain of $-60dB$ in cellular communication means that one million antennas are needed to collect all the transmitted energy. In summary, it can be said that the limit value $M \to \infty$ cannot be physically achieved, but asymptotic analysis is suitable for investigating the behavior of a system that uses many antennas.

Uplink Space-Division Multiple Access: SDMA was designed in the late 1980s and early 1990s [38, 39] and uses multiple antennas in the BS to handle causer interference in the cell. Suppresses interference due to spatial processing. In the 1990s, several field tests were performed using (at least) up to 10 antennas [34, 40]. The information-theoretic performance of these systems was characterized in the early $2000s$ and described in [41, 42] for single-cell systems using the term MU-MIMO. Note that MIMO terms are used regardless of the number of antennas mounted on each UEs, as K UEs have multiple inputs and M BS antennas have multiple outputs. Extensions from MU-MIMO to cellular

networks have been developed and considered in articles such as [43, 44], but it is difficult to determine the exact capacity in this case.

Channel State Information: The channel response h is used by BS to process UL and DL signals. These vectors need to be estimated on a regular basis. More precisely, the channel response is typically constant over a bandwidth of hundreds of kHz for a few milliseconds. Random distributions are commonly used to model channel variability. Channel state refers to the present collection of realizations of channel responses, while CSI refers to BS's understanding of it. Although it is anticipated that the network's whole statistical CSI for the distribution of random variables is known, the instant CSI for current channel realization should be obtained at the same rate as the channel change. The main method of obtaining CSI is the pilot signal, and the predefined pilot signal is transmitted from the antenna. As shown in Figure 2.2, all other antennas in the network can receive a transmit at the same time and compare it with a known pilot signal to estimate the channel of the transmit antenna. Instead, if you need to estimate the channel response from the two transmitting antennas, you generally need two orthogonal pilot signals to separate the signals from the two antennas [45, 46]. Orthogonality is achieved by using two samples for transmission. While any number of reception antennas can concurrently listen to the pilots and estimate each one's own channel to the transmitters, the number of orthogonal pilot signals is proportionate to the number of transmit antennas..

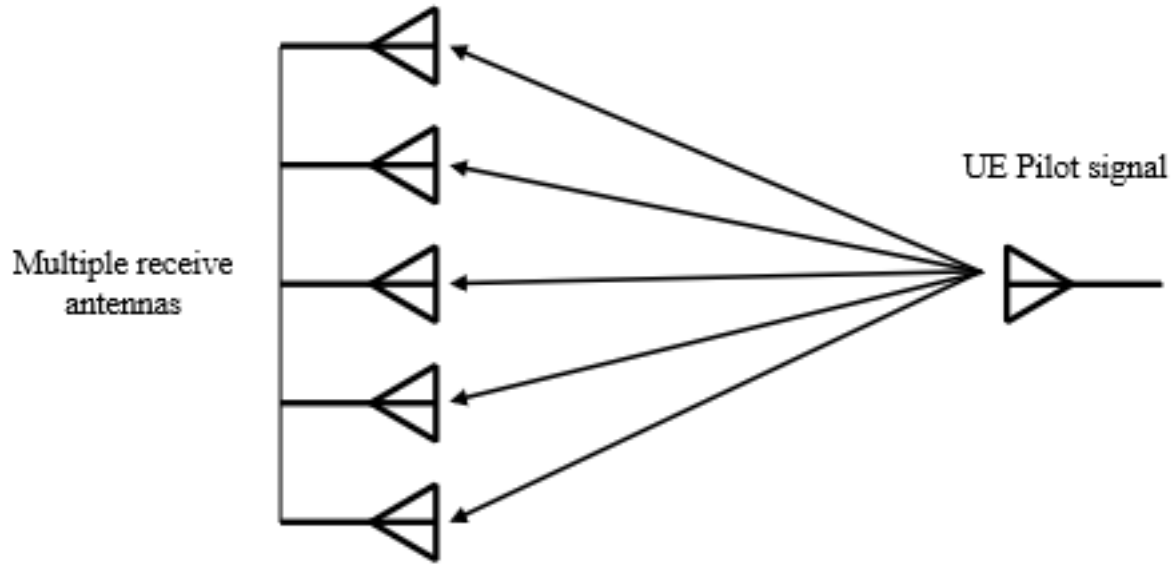

Figure 2.2: Pilot Signaling [22]

2.4 Massive MIMO

MIMO technologies have received considerable attention for modern wireless communication systems because they can substantially increase the performance targets mentioned section 1.1 [47, 48]. Recently, a MU-MIMO technology called M-MIMO, which have M active antenna elements at the BS and utilize this to communicate with single antenna

K terminals over the same time and frequency resources gain substantial interest from academia and industry [4]. The number of antennas at the BS exceeds the number of UEs units in the cell ($^{M}/_{K} \geq 1$). To satisfy the growing traffic needs of 5G wireless communication networks, the M-MIMO technology demand has increase [7, 12]. M-MIMO has long been seen to be a good way to improve both spectrum and energy efficiency in wireless communication systems. As a result, they outperform traditional MIMO systems substantially [49].

M-MIMO have the following technological characteristics; Fully digital processing, reciprocity of propagation and TDD operation, computationally inexpensive precoding/decoding algorithms, Array gain, Channel hardening, uniformly good quality of service to all terminals in a cell, and Autonomous operation of the base stations [4, 12].

2.4.1 Operational Limits of Massive MIMO

M-MIMO is scalable in terms of antennas; more antennas are always beneficial. Mobility sets the upper limit: every coherence period (coherence time multiplied by coherence bandwidth) must include UL pilots as well as payload in both the UL and DL directions. The greater the mobility, the lower the channel coherence and the fewer pilots that can be supported. This restricts the multiplexing advantage to a few dozen terminals in high-movement macro-cellular contexts, but in situations with reduced or no mobility, hundreds or even thousands of terminals might theoretically be multiplexed. In macro-cellular applications, the number of antennas that eventually prove viable is likely to be restricted to one or a few hundred, but thousands in low-mobility applications [50].

2.5 Propagation Channel

For effective utilization of the massive number of antennas at the BS, the BS should know the propagation channel between the BS and the UEs. The mobile wireless channels are characterized by their dispersiveness, the channel strength varies over time and frequency. The variation can be categorized in two ways [51]:

- **Large-scale fading:** due to path loss of signal as a function of distance and shadowing by large objects such as buildings and hills. This occurs as the mobile moves through the order of the cell size and is typically frequency-independent.
- **Small-scale fading:** due to the constructive and destructive interference of the multiple signal paths between the transmitter and receiver. This occurs at the spatial scale of the order of the carrier wavelength and is frequency-dependent.

The wireless channel has several complex-valued samples that describe the signal per second which is equal to bandwidth B. As the bandwidth increases thus time interval between two samples decreases. Since the channel is dispersive, the transmitted signal energy spreads out in each time interval and is received over a longer interval of time. When the sample interval is shorter than the spreading of the signal energy there will be substantial overlapping at the receiver side [11, 22]. This makes it hard to estimate the channel and cause inter-sample interference because the channel has memory. A conventional solution is dividing the bandwidth into many subcarriers, each carrier having a sufficiently narrow bandwidth. As result, the channel dispersion between samples is much smaller than the effective time interval. Then subcarrier channels are becoming

essentially memoryless and we can apply the spectral efficiency analysis (information-theoretic results) [11, 17, 22].

From a Massive MIMO perspective, it is not the selection of multicarrier modulation scheme is important, but the frequency resources are divided into flat fading subcarriers. The frequency interval over which the channel response is approximately constant is called ***coherence bandwidth***. Either one or multiple subcarriers fit(s) into the coherence bandwidth, thus the channel observation on two adjacent subcarriers are either closely related through a deterministic transformation or approximately equal. Hence, in general, no need to estimate the channel on every subcarrier. Similarly, in between adjacent samples, the time variance of the channel is small and the time interval over which the channel response is approximately constant is known as ***coherence time*** [11, 17].

The block over which the channel response is flat-fading and time-invariant is called ***coherence block***. For coherence time T_c and coherence bandwidth B_c, then each coherence block contains complex-valued samples τ_c [11].

The idea of coherence block and multicarrier modulation are illustrated in Figure 2.3. Since the fading channel are described by stationary ergodic random process, the channel response of a given coherence block is statistically identical to any of other coherence block, irrespective of separated either in time or frequency or in both time and frequency [11, 52]. Thus, the performance analysis we will perform in this research carried out on single statistically representative coherence block. There is an assumption that we consider, the channel realizations in pair of any coherence block are independent, which is known as **block fading assumption**.

Each coherence block operated in TDD mode (the channel estimated in the UL will be used for the DL) and Figure 2.3 illustrates how the τ_c samples are in the time and frequency plane. From given τ_c samples, τ_p UL pilots are reserved for pilot signaling, τ_u UL data for data transmissions in the UL signals and the rest of the coherence block τ_d DL is reserved for DL data transmission [11, 52]. The sum of all these three discrete

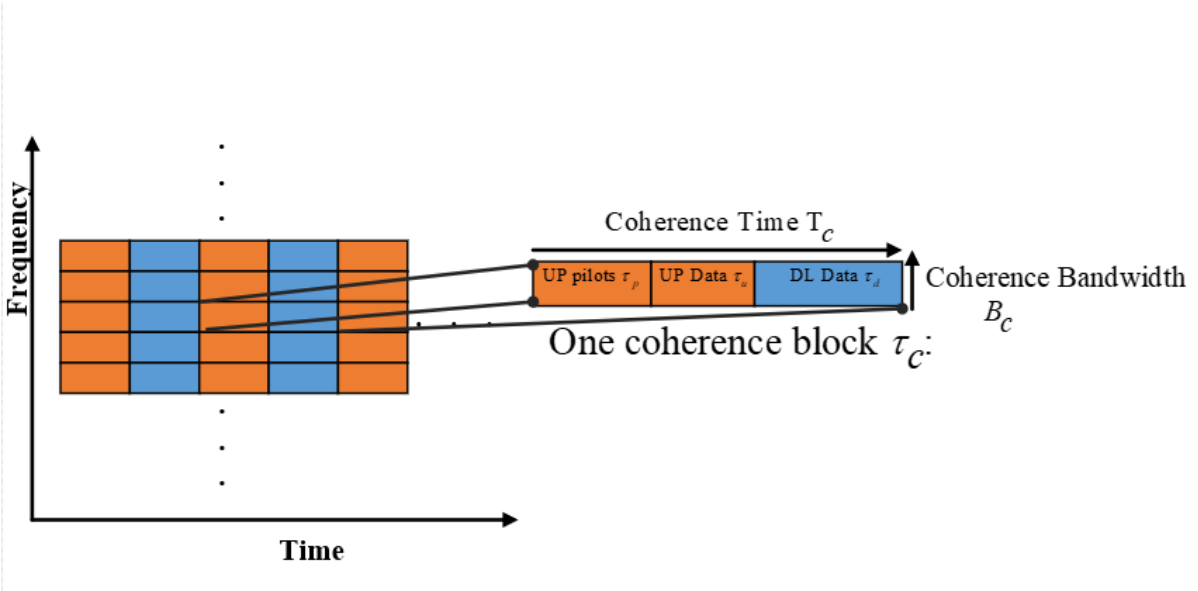

Figure 2.3: Principle of Coherence Block [4]

samples produces the size of single coherence block.

The number of pilots per coherence block is a design element, but the percentage of UL and DL data may be chosen based on network traffic statistics. Many user applications (for example, video streaming and web surfing) create DL traffic, which may be handled by using the $\tau_d > \tau_u$ option. The coherence block size constrained by the propagation environment, mobility of UEs, and carrier frequency [11, 22, 52]. Every UEs holds own coherence block, but dynamically adapting these values is hard for the network, since protocols applied to all equipment should be the same. An adapted solution is to dimension the coherence block for the worst-case propagation scenario that the network should support. The UEs does not have to send pilots in every coherence block, if it has a much larger coherence time/bandwidth [11, 22].

Because the dimensionality of the coherence block is dependent on numerous physical elements, it is difficult to have an exact measurement, although there is a general rule of thumb [53]. Coherence time T_C is the period during which UEs mobility has no effect on the phase and amplitude of a fading channel. $T_C = {}^{\lambda}/_{(4v)}$, where v is the UEs velocity, may be estimated as the time it takes to move a significant proportion of the wavelength λ. As a result, in the traditional cellular frequency range of $1 - 6\ GHz$, the coherence time is inversely related to the carrier frequency, and the channels must be estimated less often than in the Millmeter Wave (mmWave) frequency range of $30 - 300\ GHz$. Phase differences in multipath propagation determine the coherence bandwidth. $\mathrm{B}_C = {}^{1}/_{(2T_d)}$, where T_d is the delay spread, is a good approximation.

2.6 Spatially Correlated Channels

The channel between a BS with M antennas and UEs with single-antenna can be represented by an M dimensional channel vector $\mathbf{h}$. The channel between BS j and the user equipment k that are in cell l represented by $\mathbf{h}_{lk}^{j}$. The channel $\mathbf{h}_{lk}^{j} \in \mathbb{C}^M$ characterized by its norm $\|\mathbf{h}_{lk}^{j}\|^2$ and its direction ${}^{\mathbf{h}_{lk}^{j}}/_{\|\mathbf{h}_{lk}^{j}\|}$ in the vector space. Both modeled as random variables in a fading channel.

If the channel gain $\|\mathbf{h}_{lk}^{j}\|^2$ and the channel direction ${}^{\mathbf{h}_{lk}^{j}}/_{\|\mathbf{h}_{lk}^{j}\|}$ are independent random variables, and the channel direction distributed uniformly over the unit-sphere in $\mathbb{C}^M$ then the channel is spatially uncorrelated fading channel. Otherwise, the channel spatially correlated. We can observe that, the conditions for channel to be spatially uncorrelated are very strict. From these conditions we can observe that, all practical channels are spatially correlated also known as having space-selective fading [54]. There are (at least) three physical explanations for spatial correlation [12]:

- Some spatial directions contribute more multipath components to the BS than others.
- The BS antennas have spatially dependent antenna patterns and varying polarization.
- Spatially under or oversampling caused by the array geometry.

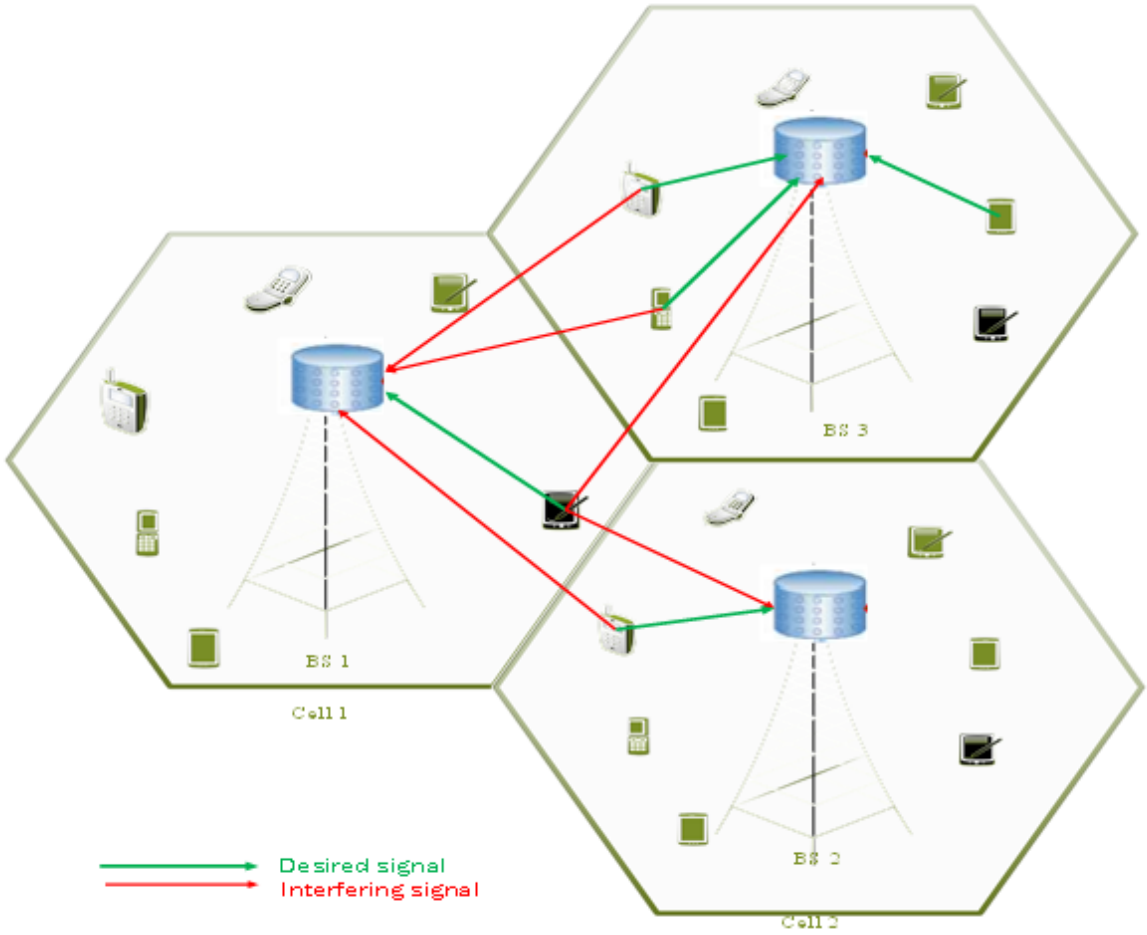

Figure 2.4: Multi-Cell Communications [3]

2.7 UpLink Transmission

Every BS must estimate the channel characteristics of each UEs in a designated region to make optimal use of antenna. Apart from pilot assignment and potentially power control, the operations in the individual cells are synchronized, but there is no cell-to-cell collaboration. Each BS is responsible for its own set of UEs. The activities of data transmission are identical to those of single-cell counterparts. However, the channel estimate must account for pilot reuse in other cells. Per coherence block, an estimation is made. The estimation is done in hexagonal cell format, as illustrated in Figure 2.4, with the assumption that all user terms in the system are synchronized.

The home cell is denoted by the index j throughout this chapter. Although each cell's terminals have mutually orthogonal pilots, some pilot reuse is allowed from cell to cell. The assumption is that the pilot sequences are either absolutely orthogonal from cell to cell or perfectly duplicated for any two unique cells. Pilot contamination occurs when cells employ the same pilots as the host cell. These cells are referred to as contaminating cells, and the collection of their indices is denoted by $\mathcal{P}_l$, which by definition includes the home cell j. The kth terminal in the lth cell is allocated the identical kth pilot sequence for every $j \in \mathcal{P}_l$.

UL transmission is a transmission from the UEs to the BS from a cellular standpoint.

We shall drive the UL transmission signal at the base station BS, as shown in Figure 2.4 The received UL signal $y_j \in \mathbb{C}^{M_j}$ at BS j is modeled as [22]

$$\mathbb{Y}_j = \sum_{l=1}^{L}\sum_{k=1}^{K_l} \mathbf{h}_{lk}^{j} s_{lk} + \mathbf{n}_j = \sum_{k=1}^{K_j} \mathbf{h}_{jk}^{j} s_{jk} + \sum_{\substack{l=1 \\ l\neq j}}^{L}\sum_{i=1}^{K_j} \mathbf{h}_{li}^{j} s_{li} + \mathbf{n}_j \tag{2.4}$$

The intended signal appears in the first term of the right equation 2.4, inter-cell interference appears in the second, and $\mathbf{n}_j \sim N\left(0, \sigma_{ul}^2 I_{M_j}\right)$ is independent additive receiver noise with zero mean and variance σ_{ul}^2. Regardless of whether it is a random payload data signal $s_{lk} \sim N\left(0, p_{lk}\right)$ or a deterministic pilot signal with $p_{lk} = |s_{lk}|^2$, the UL signal $s_{lk} \in \mathbb{C}$ from UEs k in cell l has power $p_{lk} = \mathbb{E}\left\{|s_{lk}|^2\right\}$. $\mathbf{h}_{lk}^{j} s_{lk}$ is a Rayleigh distributed function.

2.7.1 UpLink Pilot Signaling

Each BS must know the channel responses from the UEs operating in the current coherence block in order to make optimal use of the massive number of antennas. Estimates of the channels from the UEs in cell j are especially significant for BS j. Interference suppression during data transmission can also benefit from channel estimations from interfering UEs in neighboring cells.

In each coherence block, UL pilot signaling is reserved with τ_p samples from parts of the coherence block. A pilot sequence is transmitted by each UEs that spans these τ_p samples. Pilot sequence for $k's$ UEs in cell j is referred to as $\phi_{jk} \in \mathbb{C}^{\tau_p}$. To get a constant power level, it is expected to have unit-magnitude elements, which indicates that $\|\phi_{jk}\|^2 = \phi_{jk}^H \phi_{jk} = \tau_p$. The components of ϕ_{jk} are scaled as $\sqrt{p_{jk}}$ by the UL transmit power and then broadcast as the signal s_{jk} across τ_p UL samples, resulting in the received UL signal $\mathbf{Y}_j^p \in \mathbb{C}^{M_j \times \tau_p}$. This signal is given by;

$$\mathbf{Y}_j^p = \sum_{k=1}^{K_j} \sqrt{p_{jk}} \mathbf{h}_{jk}^{j} \phi_{jk}^T + \sum_{\substack{l=1 \\ l\neq j}}^{L}\sum_{i=1}^{K_j} \sqrt{p_{li}} \mathbf{h}_{li}^{j} \phi_{li}^T + \mathbf{N}_j^p \tag{2.5}$$

Where $\mathbf{N}_j^p \in \mathbb{C}^{M_j \times \tau_p}$ is independent additive receiver noise with Independently and Identically Distributed (I.I.D) elements distributed as $N_{\mathbb{C}}\left(0, \sigma_{ul}^2\right)$. The observation that BS j can use to estimate channel responses is $\mathbf{Y}_j^p$. The BS has to know which pilot sequence a certain UEs has sent in order to estimate the channel. This is why the pilot sequences are deterministic, and the pilot assignment is usually determined when the UEs connects to the BS.

Assume that BS j attempts to estimate the channel $\mathbf{h}_{li}^{j}$ from an arbitrary UEs i in cell l. After then, the BS can multiply or correlate $\mathbf{Y}_j^p$ with this UEs pilot sequence ϕ_{li}, resulting in to the processed received pilot signal $\mathbf{Y}_{jli}^p \in \mathbb{C}^{M_j}$

$$\mathbf{Y}_{jli}^p = \mathbf{Y}_j^p \phi_{li}^* = \sum_{l'=1}^{L}\sum_{i'=1}^{K_{l'}} \sqrt{p_{l'i'}} \mathbf{h}_{l'i'}^{j} \phi_{l'i'}^T \phi_{li}^* + \mathbf{N}_j^p \phi_{li}^* \tag{2.6}$$

which has the same dimension as $\mathbf{h}_{li}^{j}$. For the kth UE in the BS's own cell can be expressed as

$$\mathbf{Y}_{jjk}^{p} = \mathbf{Y}_{j}^{p}\phi_{jk}^{*} = \sqrt{p_{jk}}\mathbf{h}_{jk}^{j}\phi_{jk}^{T}\phi_{jk}^{*} + \sum_{\substack{i=1 \\ i\neq k}}^{K_j}\sqrt{p_{ji}}\mathbf{h}_{ji}^{j}\phi_{ji}^{T}\phi_{jk}^{*} + \sum_{\substack{l=1 \\ l\neq j}}^{L}\sum_{i=1}^{K_l}\sqrt{p_{li}}\mathbf{h}_{li}^{j}\phi_{li}^{T}\phi_{jk}^{*} + \mathbf{N}_{j}^{p}\phi_{li}^{*}$$

interference's are represented by the second and third terms, which comprise inner products of the type $\phi_{ji}^{T}\phi_{jk}^{*}$ between the pilot of the desired UEs and the pilot of another UEs i in cell l. The equivalent interference term in equation 2.6 disappears and has no effect on the estimate if the pilot sequences of two UEs are orthogonal (i.e., $\phi_{ji}^{T}\phi_{jk}^{*} = 0$). Since the pilots are τ_p dimensional vectors, we can only identify a collection of at most τ_p mutually orthogonal sequences for a given τ_p. The restriction $\tau_p \leq \tau_c$ is imposed by the short length of the coherence blocks, which renders assigning mutually orthogonal pilots to all UEs impractical in practice. It is difficult to maximize the pilot length since longer pilots result in fewer samples for data transmission; nonetheless, a general guideline is that τ_p should always be less than $\tau_c/2$ [55].

The network is assumed to use a set of τ_p mutually orthogonal pilot sequences. These may be collected as the columns of the UL pilot book $\mathbf{\Phi} \in \mathbb{C}^{\tau_p \times \tau_p}$, which meets the UL condition $\mathbf{\Phi}^{H}\mathbf{\Phi} = \tau_p$. It is encouraged, but not required, to have $\tau_p \geq max\{K_l\}$ pilots so that each BS can assign distinct UL pilot sequences to its UEs. The basis for this belief is because the most powerful interference generally comes from within the cell itself.

We define the set with the indices of all UEs that utilize the same pilot sequence as UEs k in cell j

$$\mathcal{P}_{jk} = \{(l,i) : \phi_{li} = \phi_{jk} \quad l = 1,2,3,\ldots,L, \quad i = 1,2,3,\ldots,K_l\}$$

Hence, $(l,i) \in \mathcal{P}_{jk}$ implies that UE k in cell j uses the same pilot as UE i in cell l. Note that $(j,k) \in \mathcal{P}_{jk}$ by definition. Using notation in the above, the expression in equation 2.6 simplifies to

$$\mathbf{Y}_{jjk}^{p} = \sqrt{p_{jk}}\tau_p\mathbf{h}_{jk}^{j} + \sum_{(l,i)\in\mathcal{P}_{li}\setminus(j,k)}\sqrt{p_{li}}\tau_p\mathbf{h}_{li}^{j} + \mathbf{N}_{j}^{p}\phi_{jk}^{*} \tag{2.7}$$

Because these UEs utilize the same pilot, $\mathbf{Y}_{jjk}^{p} = \mathbf{Y}_{jli}^{p}$ for every $(l,i) \in \mathcal{P}_{jk}$. We also observe that $\mathbf{N}_{j}^{p}\phi_{jk}^{*} \sim N_{\mathbb{C}}\left(0_{M_j}, \sigma_{ul}^{2}\tau_p I_{M_j}\right)$, since the pilot sequences are deterministic and $\|\phi_{jk}\|^2 = \tau_p$. When compared to utilizing the initially received signal $\mathbb{Y}_{j}^{p}$ [56], the processed received signal $\mathbf{Y}_{jjk}^{p}$ in 2.7 is an adequate statistic for calculating $\mathbf{h}_{jk}^{j}$ since there is no loss of important information. The rationale for this is because the required component $\mathbf{h}_{jk}^{j}\phi_{jk}^{T}$ in $\mathbf{Y}_{j}^{p}$ may be recovered from $\mathbf{Y}_{jjk}^{p}$ by multiplying with ϕ_{jk}^{T} from the right, while the interfering terms are either zero or recoverable in the same way. Similarly, for calculating $\mathbf{h}_{li}^{j}$, $\mathbf{Y}_{jli}^{p}$ is an adequate statistic [11, 22].

2.8 Channel Estimation

Every BS must estimate the channel characteristics of each UEs in a designated region to make optimal use of antenna. Apart from pilot assignment and potentially power control, the operations in the individual cells are synchronized, but there is no cell-to-cell collaboration. Each BS is responsible for its own set of UEs. The activities of

data transmission are identical to those of single-cell counterparts. However, the channel estimate must account for pilot reuse in other cells. Per coherence block, an estimation is made. The estimation is done in hexagonal cell format, as illustrated in Figure 2.4, with the assumption that all user terms in the system are synchronized.

The home cell is denoted by the index j throughout this chapter. Although each cell's terminals have mutually orthogonal pilots, some pilot reuse is allowed from cell to cell. The assumption is that the pilot sequences are either absolutely orthogonal from cell to cell or perfectly duplicated for any two unique cells. Pilot contamination occurs when cells employ the same pilots as the host cell. These cells are referred to as contaminating cells, and the collection of their indices is denoted by $\mathcal{P}_l$, which by definition includes the home cell j. The kth terminal in the lth cell is allocated the identical kth pilot sequence for every $j \in \mathcal{P}_l$.

2.9 Channel Hardening

Channel hardening is a behavior of channel that a fading channel act as a non-fading channel. In other word a fading channel behave as deterministic, while the randomness of the channel is still there. This property lightens the requirement of combating small-scale fading and negligible impact on communication channel [11, 22]. The mathematical representation for a given propagation channel $\mathbf{h}_{jk}^{j}$ provides asymptotic channel hardening if:

$$\frac{\left\|\mathbf{h}_{jk}^{j}\right\|^{2}}{\mathbb{E}\left\{\left\|\mathbf{h}_{jk}^{j}\right\|^{2}\right\}} \rightarrow 1, \text{ as } \mathrm{M}_{j} \rightarrow \infty \tag{2.8}$$

The mathematical description defined as, for arbitrary fading channel $\mathbf{h}_{jk}^{j}$ as number of antennas at the BS increase infinitely, instantaneous value of channel gain $\left\|\mathbf{h}_{lk}^{j}\right\|^{2}$ approaches to its mean value $\mathbb{E}\left\{\left\|\mathbf{h}_{lk}^{j}\right\|^{2}\right\}$

2.10 Favorable Propagation

The directions of two UEs channels become asymptotically orthogonal due to favorable propagation. This characteristic makes it easier for the BS to reduce interference between these UEs, improving the SE and allowing linear combining and precoding to be used. The pair of channels $\mathbf{h}_{jk}^{j}$ and $\mathbf{h}_{li}^{j}$ to BS j provide asymptotically favorable propagation if:

$$\frac{\left(\mathbf{h}_{jk}^{j}\right)\left(\mathbf{h}_{li}^{j}\right)}{\sqrt{\mathbb{E}\left\{\left\|\mathbf{h}_{jk}^{j}\right\|^{2}\right\}\mathbb{E}\left\{\left\|\mathbf{h}_{li}^{j}\right\|^{2}\right\}}} \rightarrow 0, \ as \ \mathrm{M}_{j} \rightarrow \infty \tag{2.9}$$

The inner product of the normalized channels $\left(\mathbf{h}_{li}^{j}\right)/\sqrt{\mathbb{E}\left\{\left\|\mathbf{h}_{li}^{j}\right\|^{2}\right\}}$ and $\left(\mathbf{h}_{jk}^{j}\right)/\sqrt{\mathbb{E}\left\{\left\|\mathbf{h}_{jk}^{j}\right\|^{2}\right\}}$ tends asymptotically to zero [11,22] according to this definition. Because the channel norms grow with M_j, favorable propagation does not imply that the inner product of $\mathbf{h}_{jk}^{j}$ and $\mathbf{h}_{li}^{j}$ approaches zero; that is, the channel directions but not the channel responses become orthogonal.

2.11 DownLink Transmission

A flexible approach for signal transmission from an array of M antennas to one or many users is transmitting precoding (beamforming). The purpose of wireless communications is to boost signal power to the intended user while reducing interference to non-intended users. To produce a high signal strength, all antennas broadcast the same data signal, but with varied amplitudes and phases, such that the signal components accumulate coherently to the user. The signal components are made to add destructively to non-intended users to achieve low interference. This is equivalent to constructing beamforming vectors (that define amplitudes and phases) with big inner products for intended channels and tiny inner products for non-intended user channels. Since transmit precoding concentrates signal energy in specific locations, less energy reaches other locations. This enables so-called SDMA, in which K geographically dispersed users be serviced concurrently. Each user is given one beamforming vector that may be matched to a channel. Unfortunately, the limited number of transmit antennas provides only a limited amount of spatial directivity, resulting in energy leakages between users that act as interference. While it is relatively simple to design a beamforming vector that optimizes signal power to the target user, striking the proper balance between signal power maximization and interference leakage is still challenging. Precoding methods are divided in to linear and non-linear precoding categories. MMSE, MRT, ZF, RZF are examples of linear precoding, while Dirty Paper Coding (DPC), Tomlinson-Harashima Precoding (THP), and Vector Perturbations (VP) are examples of non-linear precoding. In the downlink, the performance of several linear precoding algorithms will be tested.

A DL transmission is one that is sent from the BS to the UEs. While, the reverse transmission refers to the UL transmission. DL precoding is a strategy that takes use of broadcast diversity by weighting the data stream (i.e., the transmitter delivers the coded data to the recipient to achieve channel pre-information). This strategy will lessen the communication channel's contaminated effect. We will examine the feasible DL SEs based on the channel estimation we will obtained in the section 3.3.

Referring Figure 2.4, The received signal $y_{jk} \in C$ at UE k in cell j is modeled as

$$y_{jk} = \sum_{l=1}^{L} \left(\mathbf{h}_{jk}^{l}\right)^{H} \mathbf{x}_l + \mathbf{n}_{jk} = \sum_{l=1}^{L} \sum_{i=1}^{K_j} \left(\mathbf{h}_{jk}^{l}\right) \mathbf{W}_{li} \varsigma_{li} + \mathbf{n}_{jk} \tag{2.10}$$

Where

$$\mathbf{x}_l = \sum_{i=1}^{K_l} \mathbf{W}_{li} \varsigma_{li}$$

$\varsigma_{lk} \sim N_C\left(0, \rho_{lk}\right)$ is the DL data signal for UE k in the cell and ρ_{lk} is the signal power. This signal is allocated to the transmit precoding vector $\mathbf{W}_{lk} \in C^{M_l}$, which affects the transmission's spatial directivity. The precoding vector meets $\mathbb{E}\left\{\left\|\mathbf{W}_{lk}\right\|^2\right\} = 1$, hence $\mathbb{E}\left\{\left\|\mathbf{W}_{lk}\varsigma_{lk}\right\|^2\right\} = \rho_l k$ is the transmit power assigned to this UE. $\mathbf{n}_{jk} \sim N\left(0, \sigma_{DL}^2\right)$ represents independent additive receiver noise with variance σ_{DL}^2. Within a coherence block, the channels remain consistent, but the signals and noise change with each sample. Then the received signal will be:

$$y_{jk} = \left(\mathbf{h}_{jk}^{j}\right) \mathbf{W}_{jk} \varsigma_{jk} + \sum_{\substack{i=1 \\ i \neq k}}^{K_j} \left(\mathbf{h}_{jk}^{j}\right)^{H} \mathbf{W}_{ji} \varsigma_{ji} + \sum_{\substack{l=1 \\ l \neq j}}^{L} \sum_{i=1}^{K_j} \left(\mathbf{h}_{jk}^{l}\right) \mathbf{W}_{li} \varsigma_{li} + \mathbf{n}_{jk} \tag{2.11}$$

From TDD concept, the UL and DL channels are reciprocal within a coherence block, allowing the BS to use the UL channel estimations for precoding vector computation/selection. The required signal to UE k in cell j travels through the precoded channel $g_{jk} = \left(\mathbf{h}_{jk}^{j}\right)^{H} \mathbf{W}_{jk}$. The UE does not know g_{jk} a priori, but may either approximate it with the mean value $\mathbb{E}\left\{\|g_{jk}\|\right\} = \mathbb{E}\left\{\| \left(\mathbf{h}_{jk}^{j}\right)^{H} \mathbf{W}_{jk}\| \right\}$ or estimate it from received DL signals. When the lower bound of spectral efficiency derived based on approximation of g_{jk} using mean value, we call it hardening bound. Only when the precoded channel is almost predictable and the changes are minimal makes reception without immediate CSI sense. Under channel hardening, this is roughly the case, however there is usually a performance cost. The loss increases as the channel changes, and it is especially substantial for certain sorts of channels that show little or no hardening [18]. In this research, we look at estimating approach for estimating precoded channel realizations at the UEs. Because the precoded channel g_{jk} is constant inside a coherence block, UE k in cell j may estimate it without transmitting any DL pilots using the received DL signals. [18] provides an explicit technique for such estimate, but here we shall derive a lower constraint on the DL capacity that implicitly accounts for the acquisition of the precoded channels. We apply the bounding approach from [57] to the multicell case in this paper and get the following result, which we refer to as the estimation bound.

Assume that each BS computes its precoding vectors using just its own channel estimates $\mathbf{h}_{li}^{j}$ for all l and i, the DL ergodic channel capacity of UE k in cell j is lower bounded by SE_{jk}^{DL} in $\left[\frac{\frac{bit}{s}}{Hz}\right]$ [22].

$$\mathbf{SE}_{jk}^{\mathrm{DL}} = \frac{\tau_d}{\tau_c}\mathbb{E}\left\{log_2\left(1+\mathbf{SINR}_{jk}^{\mathrm{DL}}\right)\right\} - \sum_{i=1}^{K_j}\frac{1}{\tau_c}\left(\log_2\left(1+\frac{\rho_{ji}\tau_d\mathbb{V}\left\{\mathbf{W}_{ji}^{H}\mathbf{h}_{jk}^{j}\right\}}{\sigma_{\mathrm{DL}}^{2}}\right)\right) \quad (2.12)$$

$$\mathbf{SINR}_{jk}^{\mathrm{DL}} = \frac{\rho_{jk}\left|\mathbf{W}_{jk}^{H}\mathbf{h}_{jk}^{j}\right|^{2}}{\sum_{i=1}^{K_j}\rho_{ji}\left|\mathbf{W}_{ji}^{H}\mathbf{h}_{jk}^{j}\right|^{2} + \sum_{\substack{l=1\\ l\neq j}}^{K_l}\sum_{i=1}^{K_l}\rho_{li}\left|E\left\{\left(\mathbf{W}_{li}^{j}\right)^{H}\mathbf{h}_{jk}^{l}\right\}\right|^{2} + \sigma_{Dl}^{2}}$$

The first term in 2.12 can be referred to as SE with perfect intra-cell CSI, since it denotes the SE that can be obtained if the receiving UE is aware of the precoded intra-cell channels $\mathbf{W}_{jk}^{H}\mathbf{h}_{jk}^{j}$ for $i = 1, \ldots, K_j$. Because it compensates for the UE's inadequate intra-cell CSI, the second term is called CSI uncertainty loss, which is dependent on τ_d and τ_c, and it tends to zero as τ_c grows, even if τ_d increases as well (recall that $\tau_d \leq \tau_c$)). This shows that when DL transmission is done with a large coherence block, the UE can accurately estimate the precoded channel [58]. Since the capacity is unknown, the best performance indication we have is the lower bound that produces the greatest value. We shall prove numerically that when utilizing precoding algorithms that create less interference, the estimation bound provides bigger values.

Chapter 3

System Model

3.1 Introduction

In MU-MIMO spatial correlation is important property, we will now develop spatial correlation channel model that will be used in the numerical analysis of subsequent section for this research. The azimuth angle of UEs will be a parameter for the sub spaces of the correlation matrices, will help to determine if two UEs are spatially separable by comparing their respective angles.

3.2 Local Scatter Channel Modeling

In MU-MIMO spatial correlation is important property, we will now develop spatial correlation channel model that will be used in the numerical analysis of subsequent section for this research. The azimuth angle of UEs will be a parameter for the sub spaces of the correlation matrices, will help to determine if two UEs are spatially separable by comparing their respective angles [17].

Developing a model for the spatial correlation matrix $\mathbf{R} \in \mathbb{C}^{M \times M}$ for NLoS channel between a BS equipped with a Uniform Linear Array (ULA) and a UEs is our target. To make simple we drooped the indices of UEs and the signal at the receiver BS is the superposition of N_{path} multipath components, where N_{path} is a large number. Consider Figure 3.1 that, the scattering is localized around the UEs only, due to elevation at the BS there is no scattering in its near-field [17, 22]. Every component of the multipath results in a plane wave will reach the array from a particular angle $\bar{\varphi}_n$ and gives the array response $\mathbf{a}_n \in \mathbb{C}^M$:

$$\mathbf{a}_n = \mathrm{g}_n \begin{bmatrix} 1 & e^{2\pi j d_H sin\bar{\varphi}_n} & \dots & e^{2\pi j d_H (M-1) sin\bar{\varphi} n} \end{bmatrix}^T \tag{3.1}$$

where $\mathrm{g}_n \in \mathbb{C}$ represents for the gain and phase-rotation for this path and d_H stands for spacing among antennas in the array (measured in number of wavelengths). The superposition of the array response of the N_{path} components are the channel response $\mathbf{h}$ at the BS.

$$\mathbf{h} = \sum_{n=1}^{\mathrm{N}_{path}} \mathbf{a}_n \tag{3.2}$$

Assume that the angles $\bar{\varphi}_n$ I.I.D random variables with the angular Probability Density Function (PDF) $f(\bar{\varphi})$ and g_n are I.I.D. random variables with zero-mean and variance $\mathbb{E}\{|g_n|^2\}$. The variance denotes the average gain of the nth path, where as

$$\beta = \sum_{n=1}^{N_{path}} \mathbb{E}\left\{|g_n|^2\right\}$$

denotes the overall average gain of the multipath components. From multidimensional central limit theorem for infinite number of paths, it converges in distribution

$$\mathbf{h} = \sum_{n=1}^{N_{path}} \mathbf{a}_n = N_c(\mathbf{0}, \mathbf{R}) \text{ as } N_{path} \to \infty \tag{3.3}$$

where spatial correlation matrix (due to zero mean also it is covariance matrix) is

$$\mathbf{R} = \mathbb{E}\left\{\sum_n \mathbf{a}_n \mathbf{a}_n^H\right\} \in \mathbb{C}^{M \times M} \tag{3.4}$$

Positive Semi-Definite Matrix. We assumed that this matrix is known at the BS. How to estimate this matrix will be discussed in Chapter 3. Zero mean implies that there is NLoS communication between the BS and the UEs. The model is known to be as the correlated Rayleigh fading model. The channel model called Rayleigh fading, because the magnitude $\|\mathbf{h}\|$ is a Rayleigh distributed random variable.

The variations in small scale fading are modeled by Gaussian distribution. The macroscopic propagation effects, including antenna gains and radiation patterns described by

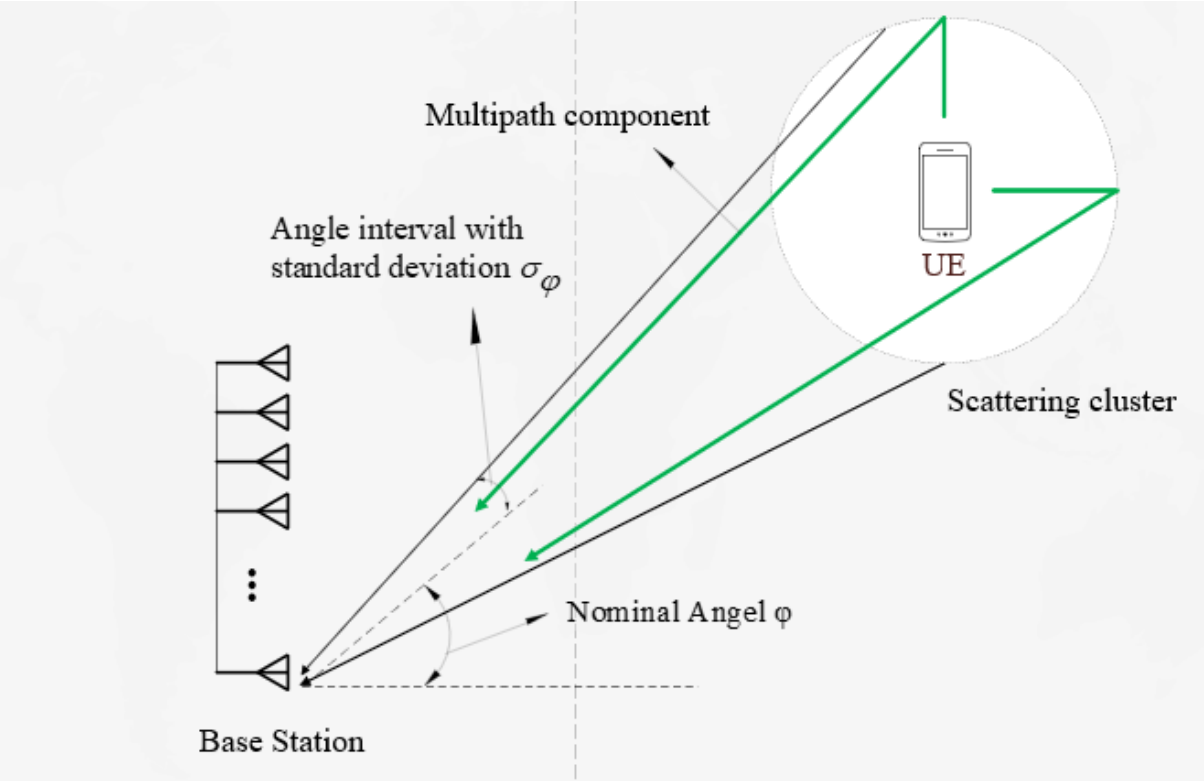

Figure 3.1: Local Scattering Channel Modeling [17]

the spatial correlation. To understand which spatial direction of channel $\mathbf{h}$ are statistically more likely to contain strong signal than the others, will be determine by the Eigenstructure of $\mathbf{R}$. Having large eigenvalue variations implies strong spatial correlation [11, 22].

The average channel gain from one of the antennas at the BS to the UEs in a given cell can also calculated as $\beta = \frac{1}{M} tr(\mathbf{R})$. M stands antenna at the BS and tr is mathematical representation of trace. In case of uncorrelated Rayleigh fading $\mathbf{R} = \beta \mathbf{I}_M$. Where $\mathbf{I}_M$ is $M \times M$ identity matrix. The parameter β is also known as large scale fading coefficient and modeled as:

$$\beta = \Upsilon - 10\alpha log_{10}\left(\frac{d}{1km}\right) + F \tag{3.5}$$

Where d is distance between transmitter and receiver, Υ represents the median channel gain at 1 km reference distance of and how fast the signal power decays with the distance determined by path-loss exponent α. According to one of the many established propagation models, we can compute the parameters Υ and α can be computed [59]. These parameters are functions of the antenna gains, carrier frequency, and vertical heights of the antennas. And all are deterministic parameters.

Shadow fading is the only non-deterministic parameter, $F = N_c\left(0, \sigma_{sf}^2\right)$, which forms a log normal distribution around the nominal value $\Upsilon - 10\alpha log_{10}\left(\frac{d}{1km}\right)$. The shadow fading can be seen as a model of physical obstruction from huge objects, or as a random adjustment term to get a model that better fits real channel measurements.

The shadow fading variance σ_{sf}^2 controls the size of random changes and is commonly expressed in terms of the standard deviation σ_{sf}. For this study, the latter is treated as a constant, but it can vary depending on the cell indices and other variables.

Recalling the correlation matrix for particular setup the (l, m)th element of $\mathbf{R}$ is

$$\begin{aligned}[\mathbf{R}]_{l,m} &= \sum_{n=1}^{\mathrm{N}_{path}} \mathbb{E}\left\{|\mathrm{g}_n|^2\right\} \mathbb{E}\left\{e^{2\pi j d_H (l-1)\sin(\bar{\varphi}_n)} e^{-2\pi j d_H (m-1)\sin(\bar{\varphi}_n)}\right\} \\ &= \beta \int e^{2\pi j d_H (l-m) sin(\bar{\varphi}_n)} f\left(\bar{\varphi}\right) d\bar{\varphi}\end{aligned} \tag{3.6}$$

Let $\bar{\varphi}$ denote the angle of an arbitrary multipath component. Numerical computation is possible for any angular distribution using the integral expression derived. We can see that $[\mathbf{R}]_{l,m}$ is Toeplitz matrix (a matrix where each descending diagonal elements from left to right are equal), since it does not depend on the individual values of l and m, but difference of $l-m$. Since we assumed that all the multipath components originate only from scattering cluster around UEs, then the angle of arbitrary multipath component is the sum of deterministic nominal angle φ and angle of random deviation δ with standard deviation σ_φ. Thus; $\bar{\varphi} = \varphi + \delta$. The channel modeling is referred as: local scattering channel modeling. Commonly the researcher followed three kinds of deviations; Gaussian distributed deviations $\delta \sim \mathcal{N}\left(0, \sigma_\varphi^2\right)$ [60–63], Laplace distributed deviations $\delta \sim Lap\left(0, \frac{\sigma_\varphi}{\sqrt{2}}\right)$ [64,65], as well as uniformly distributed deviations $\delta \sim U\left(-\sqrt{3}\sigma_\varphi, \sqrt{3}\sigma_\varphi\right)$ [66–68] can be found in the literature. Because all the scatterers may be considered to lie on a circle centered at the UEs, the latter case is also known as the one-ring model illustrated in Figure 3.1. The standard deviation called Angular Standard Deviation (ASD) because it is measured

in radians and it is always positive. Depending on the cellular network deployment area ASD σ_φ value can vary, urban case less than 10° [65], in flat rural area the smaller values are expected and larger values in hilly areas [54].

3.3 Minimum Mean-Squared Error Estimator

The purpose of channel estimation is to estimate an unknown channel variable's value based on measurements. We are especially interested in Bayesian estimation in which the unknown channel variable is a realization of a random variable with a known, or partially known, statistical distribution [22]. Let $\hat{X}(y)$ be an arbitrary estimate of x based on the observation $Y \in \mathbb{C}^T$ and consider a random variable $X \in \mathbb{C}^N$ with support in X. The estimator that minimizes the anticipated loss for a given loss function $\ell(,.,)$

$$\mathbb{E}\left\{\ell\left(X, \hat{X}(y)\right)\right\} \tag{3.7}$$

is called a Bayesian estimator [11]. There are a variety of possible loss functions, but the squared difference is of crucial concern in this research since its expectation is the estimate error variance.

The MMSE estimator is given by the loss function $\ell\left(X, \hat{X}(y)\right) = \left\|X - \hat{X}(y)\right\|^2$ and thus minimizes the MSE;

$$\mathbb{E}\left\{\left\|X - \hat{X}(y)\right\|^2\right\}$$

This research is particularly interested in the MMSE estimator of a complex Gaussian random variable from an observation contaminated by independent additive complex Gaussian noise (and interference).

Based on the received pilot signal $\mathbf{Y}_j^p$ in 2.4 and a pilot book with mutually orthogonal sequences, we will now develop an estimate of the channel response $\mathbf{h}_{li}^j$. Because the channel is a manifestation of a random variable, Bayesian estimators are preferable because they account for the statistical distributions of the variables [11]. The distributions must be known for Bayesian estimators to work.

Remember that $\mathbf{h}_{li}^j \sim N_c\left(\mathbf{0}_{M_j}, \mathbf{R}_{li}^j\right)$, the vector $\hat{\mathbf{h}}_{li}^j$ that minimizes the $\mathbb{E}\left\{\left\|\mathbf{h}_{li}^j - \hat{\mathbf{h}}_{li}^j\right\|^2\right\}$ is the MMSE estimator of $\mathbf{h}_{li}^j$ [22].
The MMSE estimate of the channel $\mathbf{h}_{li}^j$ based on the observation $\mathbf{Y}_j^p$ is [22]:

$$\hat{\mathbf{h}}_{li}^j = \sqrt{p_{li}}\mathbf{R}_{li}^j \boldsymbol{\Psi}_{li}^j \mathbf{Y}_{jli}^p \tag{3.8}$$

is calculated using a pilot book with mutually orthogonal sequences.
Where

$$\boldsymbol{\Psi}_{li}^j = \left(\sum_{(l',i') \in \mathcal{P}_{li}} p_{l'i'}\tau_p \mathbf{R}_{l'i'}^j + \sigma_{ul}^2 \mathbf{I}_{M_j}\right)^{-1} \tag{3.9}$$

The estimation error $\widetilde{\mathbf{h}}_{li}^j = \mathbf{h}_{li}^j - \hat{\mathbf{h}}_{li}^j$ has correlation matrix

$$\mathbf{C}_{li}^j = \mathbf{R}_{li}^j - p_{li}\tau_p \mathbf{R}_{li}^j \boldsymbol{\Psi}_{li}^j \mathbf{R}_{li}^j \tag{3.10}$$

This provides a technique to calculate the MMSE estimate for each UE to BS j channel in the network. The Mean Square Error (MSE), which is $\mathbb{E}\left\{\left\|\mathbf{h}_{li}^{j}-\hat{\mathbf{h}}_{li}^{j}\right\|^{2}\right\}=tr\left(\mathbf{C}_{li}^{j}\right)$.

To calculate $\mathbf{h}_{li}^{j}$ using 3.8, the BS must first correlate the received pilot signal with the pilot sequence utilized by UE i in cell l, as $\mathbf{Y}_{jli}^{p}=\mathbf{Y}_{j}^{p}\phi_{li}^{*}$, and then multiply this observation by the two matrices $\mathbf{\Psi}_{li}^{j}$ and $\mathbf{R}_{li}^{j}$. The matrix $\mathbf{\Psi}_{li}^{j}$ is the inverse of the processed received signal's normalized correlation matrix $\frac{1}{\tau_{p}}\mathbb{E}\left\{\mathbf{Y}_{jli}^{p}\left(\mathbf{Y}_{jli}^{p}\right)^{H}\right\}$, whereas $\mathbf{R}_{li}^{j}$ is the spatial correlation matrix of the channel to be estimated. Interference and noise that do not have the same second-order statistics as $\mathbf{h}_{li}^{j}$ are suppressed by these multiplications.

Note that the MMSE estimator in 3.8 is linear, as $\mathbf{h}_{li}^{j}$ is obtained by multiplying the processed received signal $\mathbf{Y}_{jli}^{p}$ with matrices. The linear MMSE estimator is the term given to the estimation shown. However, we prefer to employ the MMSE concept to emphasize that a non-linear estimator cannot further lower the MSE.

The transmit power appears solely as a product with the pilot length in the estimate error correlation matrix in 3.10 is $p_{li}\tau_{p}$. During pilot signaling from UE k in cell j to its serving BS j, we define the effective SNR as

$$\mathrm{SNR}_{jk}^{p}=\frac{p_{jk}\tau_{p}\beta_{jk}^{j}}{\sigma_{UL}^{2}} \tag{3.11}$$

The term effective SNR denotes that the SNR includes the pilot processing gain τ_{p}. Because the pilot sequence spans τ_{p} samples, the processing gain is obtained. The effective SNR is 10 dB higher than the nominal SNR for a single sample if the pilot sequences are 10 samples long. This gain is extremely desirable for UEs with low transmit power and/or poor channel circumstances to achieve decent estimate quality.

In an arbitrary coherence block, the following statistical features apply if we examine the random realizations of the MMSE channel estimate and the accompanying estimation error. The estimation error $\widetilde{\mathbf{h}}_{li}^{j}$ and the MMSE estimate $\hat{\mathbf{h}}_{li}^{j}$ are independent random variables that are distributed as follows:

$$\hat{\mathbf{h}}_{li}^{j}\sim N_{c}\left(\mathbf{0}_{M_{j}},\mathbf{R}_{li}^{j}-\mathbf{C}_{li}^{j}\right)$$

$$\widetilde{\mathbf{h}}_{li}^{j}\sim N_{c}\left(\mathbf{0}_{M_{j}},\mathbf{C}_{li}^{j}\right)$$

When we later compute the SE of each UE, the statistical distributions described come in handy. We can also see that the estimated channel's average squared norm $\mathbb{E}\left\{\left\|\hat{\mathbf{h}}_{li}^{j}\right\|^{2}\right\}=tr(\mathbf{R}_{li}^{j})-tr(\mathbf{C}_{li}^{j})$ is less than the genuine channel's, but it grows when the MSE: $tr(\mathbf{C}_{li}^{j})$ drops. We have $\mathbb{E}\left\{\left\|\hat{\mathbf{h}}_{li}^{j}\right\|^{2}\right\}=\mathbb{E}\left\{\left\|\mathbf{h}_{li}^{j}\right\|^{2}\right\}=tr(\mathbf{R}_{li}^{j})$, in the particular case of $tr\left(\mathbf{C}_{li}^{j}\right)=0$, since we achieved flawless estimation.

Inter-cell channels from any UE in the network to BS j can be approximated in practice. Comparing the MMSE estimate of an intra-cell channel $\hat{\mathbf{h}}_{jk}^{j}$ with the estimate $\hat{\mathbf{h}}_{li}^{j}$ of a UE in another cell that uses the same pilot sequence ($i.e.$, $(l,i)\in\mathcal{P}_{jk}$ which implies $\phi_{li}=\phi_{jk}$ and $\mathcal{P}_{jk}=\mathcal{P}_{li}$). Reveals an interesting finding that is $\mathbf{\Psi}_{li}^{j}=\mathbf{\Psi}_{jk}^{j}$ and $\mathbf{Y}_{jjk}^{p}=\mathbf{Y}_{jli}^{p}$. As a result, the identical matrix inverse is multiplied with the same incoming signal that

has been processed. In 3.9, just the scalar and the first matrix are different. If $\mathbf{R}_{jk}^{j}$ is invertible, we may describe the connection as

$$\hat{\mathbf{h}}_{li}^{j} = \frac{\sqrt{p_{jk}}}{\sqrt{p_{li}}} \mathbf{R}_{li}^{j} \left(\mathbf{R}_{jk}^{j}\right)^{-1} \widehat{\mathbf{h}}_{jk}^{j} \tag{3.12}$$

This means that the two estimations are tightly linked, but the vectors are normally linearly independent (i.e., non-parallel) since $\mathbf{R}_{li}^{j}$ and $\mathbf{R}_{jk}^{j}$ must be equal up to a scaling factor for $\hat{\mathbf{h}}_{li}^{j}$ to be written as a scalar times $\widehat{\mathbf{h}}_{jk}^{j}$. The two channel estimates are parallel vectors with only a scaling difference in the exceptional case of spatially uncorrelated channels with $\mathbf{R}_{li}^{j} = \beta_{li}^{j}\mathbf{I}_{M_j}$ and $\mathbf{R}_{jk}^{j} = \beta_{jk}^{j}\mathbf{I}_{M_j}$. This is an undesirable quality induced by BS j's inability to distinguish between UEs that have transmitted the same pilot sequence and have identical spatial characteristics.

Consider UE k in cell j and UE i in cell l. The correlation matrix of the respective channel estimates at BS j is [22]

$$\mathbb{E}\left\{\hat{\mathbf{h}}_{jk}^{j}\left(\hat{\mathbf{h}}_{li}^{j}\right)^{H}\right\} = \begin{cases} \sqrt{p_{li}p_{jk}}\tau_{\mathrm{p}}\mathbf{R}_{jk}^{j}\boldsymbol{\Psi}_{li}^{j}\mathbf{R}_{li}^{j} & (l,i) \in \mathcal{P}_{jk} \\ 0 & (l,i) \notin \mathcal{P}_{jk} \end{cases} \tag{3.13}$$

The antenna-averaged correlation coefficient is

$$\frac{\mathbb{E}\left\{\hat{\mathbf{h}}_{li}^{j}\left(\hat{\mathbf{h}}_{jk}^{j}\right)^{H}\right\}}{\sqrt{\mathbb{E}\left\{\left\|\hat{\mathbf{h}}_{li}^{j}\right\|^{2}\right\}\mathbb{E}\left\{\left\|\hat{\mathbf{h}}_{jk}^{j}\right\|^{2}\right\}}} = \begin{cases} \frac{tr\left(\mathbf{R}_{li}^{j}\mathbf{R}_{jk}^{j}\boldsymbol{\Psi}_{li}^{j}\right)}{\sqrt{tr\left(\mathbf{R}_{jk}^{j}\mathbf{R}_{jk}^{j}\boldsymbol{\Psi}_{li}^{j}\right)tr\left(\mathbf{R}_{li}^{j}\mathbf{R}_{li}^{j}\boldsymbol{\Psi}_{li}^{j}\right)}} & (l,i) \in \mathcal{P}_{jk} \\ 0 & (l,i) \notin \mathcal{P}_{jk} \end{cases} \tag{3.14}$$

This describes one of the fundamental features of the pilot contamination phenomena is that UEs transmitting the identical pilot sequence corrupt each other's channel estimations. The interference not only lowers estimation quality (i.e., raises the MSE), but it also renders channel estimations statistically dependent, despite the fact that the genuine channels are statistically independent. Beyond channel estimation, pilot contamination has a significant impact since it makes it difficult for the BS to control interference between UEs using the same pilot. M-MIMO's fundamental characteristic and limiting element is sometimes defined as pilot contamination. Although it was the subject of some of the early research [3, 5, 7], the phenomena is not unique to M-MIMO. Because it is necessary to reuse time-frequency resources between cells in most cellular networks, it exists. However, pilot contamination can have a higher impact on M-MIMO networks than on traditional networks. This is partly due to the increased number of UEs necessitating more frequent pilot sequence reuse in space, and partly due to the signal processing in MIMO being particularly excellent at reducing interference between UEs with orthogonal pilots.

Recall that the MMSE estimator minimizes the MSE of the channel estimate, which is defined as

$$\mathbb{E}\left\{\left\|\mathbf{h}_{li}^{j} - \hat{\mathbf{h}}_{li}^{j}\right\|^{2}\right\} = \mathbb{E}\left\{\left\|\widetilde{\mathbf{h}}_{li}^{j}\right\|^{2}\right\} = \mathbb{E}\left\{tr\left(\widetilde{\mathbf{h}}_{li}^{j}\left(\widetilde{\mathbf{h}}_{li}^{j}\right)^{H}\right)\right\} = tr(\mathbf{C}_{li}^{j})$$

The NMSE is a quality-of-estimate metric that may be used to compare the accuracy of various estimation strategies in various situations. Because it measures the relative estimate error per antenna,

$$NMSE_{li}^{j} = \frac{tr\left(\mathbf{C}_{li}^{j}\right)}{tr\left(\mathbf{R}_{li}^{j}\right)} \tag{3.15}$$

is a useful metric. This is a number between 0 (perfect estimation) and 1 (estimation based on the mean value of the variable, $\mathbb{E}\left\{\mathbf{h}_{li}^{j}\right\}$,).

3.4 Impact of Spatial Correlation

When we examine the estimate of the channel response of a UE with a unique pilot sequence, the essential features of channel estimation are best stated. Noise, not interference, is the sole factor that affects the estimate. Consider the channel $\mathbf{h} \sim N_c\left(\mathbf{0}_M, \mathbf{R}\right)$, where the UE and BS indices have been removed for brevity. Let $\mathbf{R} = \mathbf{U}\mathbf{\Lambda}\mathbf{U}^H$ signify the eigenvalue decomposition of the correlation matrix, where the eigenvectors, also known as eigendirections, are included in the unitary matrix $\mathbf{U} \in \mathbb{C}^{M\times M}$, and the corresponding eigenvalues are contained in the diagonal matrix $\mathbf{\Lambda} = diag\left(\lambda_1, \ldots, \lambda_M\right)$.

The estimation error correlation matrix in 3.9 becomes.

$$\begin{aligned}
\mathbf{C} &= \mathbf{R} - p\tau_p\mathbf{R}\left(p\tau_p\mathbf{R} + \sigma_{ul}^2\mathbf{I}_M\right)^{-1}\mathbf{R} \\
&= \left(\mathbf{\Lambda} - p\tau_p\mathbf{\Lambda}\left(p\tau_p\mathbf{\Lambda} + \sigma_{ul}^2\mathbf{I}_M\right)^{-1} + \mathbf{\Lambda}\right)\mathbf{U}^H \\
&= \mathbf{U}diag\left(\lambda_1 - \frac{p\tau_p\lambda_1^2}{p\tau_p\lambda_1 + \sigma_{ul}^2}, \ldots, \lambda_M - \frac{p\tau_p\lambda_M^2}{p\tau_p\lambda_M + \sigma_{ul}^2}\right)\mathbf{U}^H
\end{aligned}$$

Where the second equivalence is derived from the fact that $\mathbf{I}_M = \mathbf{U}\mathbf{U}^{\mathbf{H}}$ and $\mathbf{U}^{-1}\mathbf{U} = \mathbf{I}_M$. The eigenvalue decomposition with eigenvectors in U and the mth eigenvalue supplied is discovered as.

$$\lambda_M - \frac{p\tau_p\lambda_M^2}{p\tau_p\lambda_M + \sigma_{ul}^2} = \frac{\sigma_{ul}^{\mathbf{2}}\lambda_M}{p\tau_p\lambda_M + \sigma_{ul}^2} = \frac{\lambda_M}{\mathrm{SNR}^p\frac{\lambda_M}{\beta} + 1} \tag{3.16}$$

Where SNR^p denotes the effective SNR, $\beta = \frac{1}{M}tr\left(\mathbf{R}\right) = \frac{1}{M}\sum_{n=1}^{M}\lambda_n$, Because of the subtraction, the estimate error correlation matrix C has the same eigenvectors as the spatial correlation matrix $\mathbf{R}$, but the eigenvalues are different and typically lower. The estimation error variance in each eigendirection is represented by the eigenvalues of $\mathbf{C}$ in 3.16. All these error variances decrease as the effective SNR grows, approaching zero as $\mathrm{SNR}^p \to \infty$, demonstrating that error-free estimation is conceivable in this asymptotic domain. Another key finding from 3.16 is that an eigendirection of $\mathbf{R}$ with a big eigenvalue λ_M has a lower normalized error variance than one with a smaller eigenvalue;

$$\frac{\frac{\lambda_M}{SNR^p\frac{\lambda_M}{\beta}+1}}{\lambda_M} = \frac{1}{\mathrm{SNR}^p\frac{\lambda_M}{\beta} + 1}$$

The concept is that the eigendirections are estimated separately, with strong eigendirections being easier to estimate due to the greater SNR.

3.5 Channel Hardening and Favourable Propagation

Considering correlated Rayleigh fading $\mathbf{h}_{jk}^{j} \sim \mathcal{N}_{\mathbb{C}}\left(0_{M_j}, \mathbf{R}_{jk}^{j}\right)$; for asymptotic channel hardening to be observed, we have sufficient and necessary conditions. A sufficient condition is that the spectral norm $\|\mathbf{R}_{lk}^{j}\|_2$ of the spatial correlation matrix is bounded and the average channel gain $\beta_{lk}^{j} = \frac{1}{M_j} tr\left(\mathbf{R}_{jk}^{j}\right)$ remains strictly positive as $M_j \to \infty$. The necessary but not sufficient condition is the variance goes to zero. The important thing for practical purposes is, how close to asymptotic channel hardening we are with a practical number of antennas, not the asymptotic result [11, 22]. This can be quantified by considering the variance expression

$$\mathbb{V}\left\{\frac{\|\mathbf{h}_{jk}^{j}\|^2}{\mathbb{E}\left\{\|\mathbf{h}_{jk}^{j}\|^2\right\}}\right\} = \frac{\mathbb{V}\left\{\|\mathbf{h}_{jk}^{j}\|^2\right\}}{\left(\mathbb{E}\left\{\|\mathbf{h}_{jk}^{j}\|^2\right\}\right)^2} \approx \frac{tr\left(\left(\mathbf{R}_{jk}^{j}\right)^2\right)}{\left(tr\left(\mathbf{R}_{jk}^{j}\right)\right)^2} = \frac{tr\left(\left(\mathbf{R}_{jk}^{j}\right)^2\right)}{\left(M_j \beta_{jk}^{j}\right)^2} \tag{3.17}$$

The variance must approach to zero, if the channel hardening must be observed.

A sufficient condition for correlated Rayleigh fading channels is that the spatial correlation matrices $\mathbf{R}_{li}^{j}$ and $\mathbf{R}_{jk}^{j}$ have bounded spectral norms and the average channel gains $\beta_{li}^{j} = \frac{1}{M_j} tr(\mathbf{R}_{li}^{j})$ and $\beta_{jk}^{j} = \frac{1}{M_j} tr(\mathbf{R}_{jk}^{j})$ remain strictly positive as $M_j \to \infty$. The two channels will also produce asymptotic channel hardening under this scenario. Consider the variance expression to see how near we are to asymptotic favorable propagation with a reasonable number of antennas.

$$\mathbb{V}\left\{\frac{\left(\mathbf{h}_{jk}^{j}\right)\left(\mathbf{h}_{li}^{j}\right)}{\sqrt{\mathbb{E}\left\{\|\mathbf{h}_{li}^{j}\|^2\right\}\mathbb{E}\left\{\|\mathbf{h}_{jk}^{j}\|^2\right\}}}\right\} = \frac{tr\left(\mathbf{R}_{jk}^{j}\mathbf{R}_{li}^{j}\right)}{tr\left(\mathbf{R}_{jk}^{j}\right) tr\left(\mathbf{R}_{li}^{j}\right)} \tag{3.18}$$

The variance of the equation is a measurement of how orthogonal the channel directions are, which impacts how much interference the UEs cause. When using MRT combining/precoding, the inner product between the channels shows directly in the received signals, resulting in a very strong correlation [22]. The variance should be as small as possible. Because the variance in practice is non-zero, we can benefit from combining/precoding strategies that reduce inter-user interference. If both channels have uncorrelated fading, the variance becomes $1/M_j$ and reduces as the number of antennas increases. In general, the variance is determined by the spatial channel correlation. It is 0 if the UEs have orthogonal correlation eigenspaces, and it is 1if the UEs have identical eigenspaces and just a few strong eigenvalues [11, 22].

3.6 Linear Precoding Vector Design

Selecting precoding vectors is a tricky problem. This is because all precoding vectors in the network influence each UE, making network-wide precoding optimization impossible. Precoding must clearly strike a balance between selfishly directing the signal to the intended UE and altruistically avoiding interfering with other UEs [69]. Finding the correct balance between these two aims is challenging, especially when there are numerous UEs involved. As a result, having a sensible, yet tractable, precoding design principle is desirable. There are several heuristic precoding design concepts in the literature, but the

best ones are generally quite similar and tightly linked to a basic characteristic known as UL-DL duality [52, 70]. This UL-DL duality theorem indicates that if the DL combining vectors are employed as DL precoding vectors and the DL transmit power is allotted, the SE attained in the UL can also be accomplished in the DL.

For any given set of receive combining vectors $\mathbf{V}_{li}$, we can achieve

$$\mathbf{SINR}_{jk}^{UL} = \mathbf{SINR}_{jk}^{DL} \qquad j = 1, \ldots, L \quad k = 1, \ldots K_j$$

if the following condition is satisfied, precoding vectors are selected for all j and k as [22]:

$$\mathbf{W}_{jk} = \frac{\mathbf{V}_{jk}}{\mathbb{E}\left\|\mathbf{V}_{jk}\right\|}$$

3.6.1 Linear Precoding Techniques

We derived the DL SE and the UL-DL duality design of precoding vector utilizing estimated channel using MMSE estimation; in the next part, we will examine alternative linear precoding strategies.

Minimum Mean squared Error Precoding

In a M-MIMO DL system, MMSE precoding is the best linear precoding. The MSE approach is used to create this strategy. The Lagrangian optimization approach is utilized to create this precoder since average power at each transmitted antenna is restricted. First, we consider the signal's MSE. You may find this precoding techniques as Multi cell (M-MMSE) precoding to differentiate the precoding in single cell (S-MMSE) in some references, but here we consider only the precoding of multi cell scenario refer (M-MMSE) as MMSE. The MMSE precoding expression is used for the practical case when only the estimated channels are known. This precoding not only minimizes the MSE in the data transmission but also maximizes the instantaneous SINR.

Recall idea of channel estimation in chapter 2 , the UL SE in the UL with the MMSE estimation will be;

$$\mathrm{SE}_{jk}^{\mathrm{UL}} = \frac{\tau_u}{\tau_c}\mathbb{E}\left\{log_2\Big(2 + \mathrm{SINR}_{JK}^{\mathrm{UL}}\Big)\right\}\left[\frac{\frac{bit}{s}}{Hz}\right]$$

$$\mathrm{SINR}_{jk}^{\mathrm{UL}} = \frac{\rho_{jk}\left|\mathbf{V}_{jk}^H\hat{\mathbf{h}}_{jk}^j\right|^2}{\sum_{l=1}^{L}\sum_{i=1}^{K_l}\rho_{jk}\left|\mathbf{V}_{jk}^H\hat{\mathbf{h}}_{jk}^j\right|^2 + \mathbf{V}_{jk}^H\left(\sum_{l=1}^{L}\sum_{i=1}^{K_l}\rho_{li}\mathbf{C}_{li}^j + \sigma_{\mathrm{UL}}^2\mathbf{I}_{M_j}\right)\mathbf{V}_{jk}}$$

The MMSE combining vector $\mathbf{V}_{jk}^{\mathrm{MMSE}}$ that minimizes the conditional MSE, $\mathbb{E}\left\{\left|s_{jk} - \mathbf{V}_{jk}^H\mathbf{Y}_j\right|^2 \mid \left\{\hat{\mathbf{h}}_{jk}^j\right\}\right.$ is given by;

$$\mathbf{V}_{jk}^{\mathrm{MMSE}} = \left(\sum_{l=1}^{L}\hat{\mathbf{h}}_{jk}^j\rho_{jk}\left(\mathbf{h}_{jk}^j\right)^H + \sum_{l=1}^{L}\sum_{i=1}^{K_l}\rho_{li}\mathbf{C}_{li}^j + \sigma_{\mathrm{UL}}^2\mathbf{I}_{M_j}\right)^{-1}\hat{\mathbf{h}}_{jk}^j p_{jk} \tag{3.19}$$

The combining vector is the only one that minimizes the MSE, although multiplying $\mathbf{V}$ with any non-zero scalar has no effect on the instantaneous SINR (i.e., we can normalize the vector arbitrarily).

From principle of precoding design, we argued that the precoding vector is power of unit magnitude with the same vector directions of the combining vectors. Thus, the MMSE precoding will be;

$$\mathbf{W}_{jk}^{\mathrm{MMSE}} = \mathbf{v}_{jk}^{\mathrm{MMSE}} / \mathbb{E}\left\|\mathbf{v}_{jk}^{\mathrm{MMSE}}\right\|$$

Regularized Zero Forcing

We may ignore all the correlation matrices in the MMSE combing vector if BS j only estimates the channels from its own UEs [10,13,35] and assumes that the channel conditions are excellent and the interfering signals from other cells are weak.

$$\mathbf{V}_{jk}^{\mathrm{RZF}} = \hat{\mathbf{h}}_{jk}^{j}\left(\left(\hat{\mathbf{h}}_{jk}^{j}\right)^{H}\hat{\mathbf{h}_{jk}^{j}} + \sigma_{UL}^{2}\rho_{jk}^{-1}\right)^{-1} \tag{3.20}$$

The normalized version of the combing vector $\mathbf{v}_{jk}^{\mathrm{RZF}} / \mathbb{E}\left\|\mathbf{v}_{jk}^{\mathrm{RZF}}\right\|$ yield the DL precoding vector $\mathbf{W}_{jk}^{\mathrm{RZF}}$.

As a result of substantial interference signals from adjacent cells and generally unfavorable channel conditions for all UEs, this enhancement is compensated by a SE loss.

The term "regularization" indicates to the fact that equation 3.20 is a pseudo-inverse of the estimated channel matrix $\hat{\mathbf{h}}_{jk}^{j}$, where the inverted matrix is regularized by the diagonal matrix $\sigma_{ul}^{2}\rho_{jk}^{-1}$. An inverse's numerical stability is improved via regularization, a well-known signal processing technique. It strikes a compromise between signal maximization and interference reduction (for modest regularization factors) in our circumstance (for large regularization terms).

Zero Forcing

When the SNR is large, the combining expression in 3.20 can be approximated further by using the regularization term $\sigma_{ul}^{2}\rho_{jk}^{-1} \rightarrow \mathbf{0}\mathbf{I}_{Kj}$. The same approximation may be used in the situation of many antennas, where $\left(\left(\hat{\mathbf{h}}_{jk}^{j}\right)^{H}\hat{\mathbf{h}}_{jk}^{j} + \sigma_{ul}^{2}p_{jk}^{-1}\right) \approx \left(\hat{\mathbf{h}}_{jk}^{j}\right)^{H}\hat{\mathbf{h}}_{jk}^{j}$, since the diagonal of $\left(\hat{\mathbf{h}}_{jk}^{j}\right)^{H}\hat{\mathbf{h}}_{jk}^{j}$ rises with M_j while the regularization term remains constant. We may ignore the regularization term in both situations and obtain the ZF combining matrix, which is the pseudo-inverse of $\left(\hat{\mathbf{h}}_{jk}^{j}\right)^{H}$.

$$\mathbf{V}_{jk}^{\mathrm{ZF}} = \hat{\mathbf{h}}_{jk}^{j}\left(\left(\hat{\mathbf{h}}_{jk}^{j}\right)^{H}\hat{\mathbf{h}}_{jk}^{j}\right)^{-1} \tag{3.21}$$

If we compute $\left(\hat{\mathbf{h}}_{jk}^{j}\right)^{H}\mathbf{V}_{jk}$ for any combining scheme, The kth diagonal matrix reflects the intended signal gain of the kth UE in cell j, while the (k,i)th element indicates the interference that UE k causes to UE i in the same cell (for $(k \neq i)$).The combining vector in 3.21 is termed ZF, $\hat{\mathbf{h}}_{jk}^{j}\mathbf{V}_{jk}^{\mathrm{ZF}} = \mathbf{I}_{K_j}$, implying that all intra-cell UE interference is eliminated (on average), but the intended signals remain non-zero. There will be residual interference with ZF since the real channel matrix is $\mathbf{h}_{jk}^{j}$ and not $\hat{\mathbf{h}}_{jk}^{j}$. Because hardly every UE in practice has a high SNR, ZF is likely to have lower SEs than RZF.

Due to its minimal complexity, ZF precoding is a well-known MIMO precoding method, and it may be done without any prior knowledge of noise statistics. By projecting each stream onto the orthogonal complement of the inter-user interference, ZF entirely eliminates multi-user interference.

Maximum Ratio Transmission

In low SNR situations, we have $\left(\left(\hat{\mathbf{h}}_{jk}^{j}\right)^{H}\hat{\mathbf{h}}_{jk}^{j}+\sigma_{UL}^{2}\rho_{jk}^{-1}\right)\approx\sigma_{UL}^{2}\rho_{jk}^{-1}$ and RZF in 3.20 is about equivalent to $\frac{1}{\sigma_{ul}^{2}}\hat{\mathbf{h}}_{jk}^{j}\rho_{jk}$. If we remove the diagonal matrix $\frac{1}{\sigma_{ul}^{2}}\rho_{jk}$ (remember that normalizing a combining vector has no effect on the instantaneous UL SINR),

$$\mathbf{V}_{jk}^{MR}=\hat{\mathbf{h}}_{jk}^{j} \tag{3.22}$$

In contrast to the previously stated techniques, MRT does not need any matrix inversion. Because not every UE has a low SNR in practice, MRT is projected to yield lower SEs than RZF.

Chapter 4

Result and Discussion

4.1 Introduction

The findings will be generated using Matlab simulation, following the theoretical basis and design methods presented in earlier chapters. The impact of spatial correlation on channel hardening and favourable propagation is the first observation we discovered using the approach. We analyzed the impact of UEs location on channel estimation using NMSE and pilot contamination effect. The NMSE is examined in the case of both wanted and interfering UEs with different signal strengths. The last results look at the DL's spectral efficiency over different precoding schemes. The overall steps for result analysis are shown in the Flowchart 4.1.

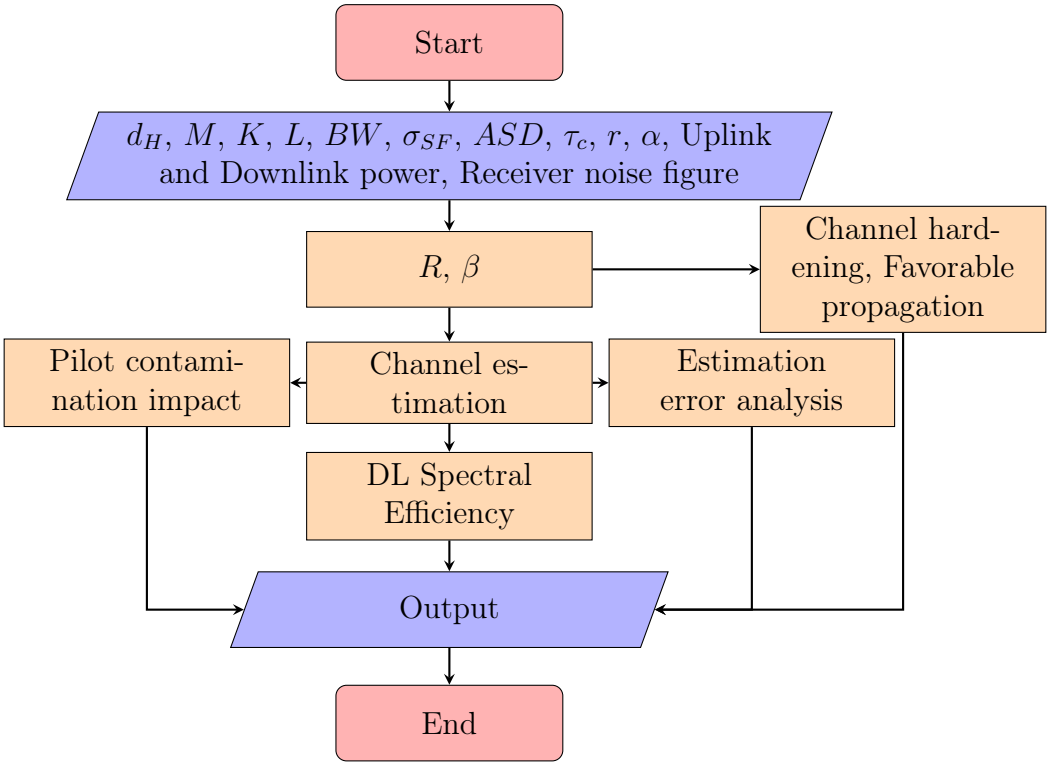

Figure 4.1: Steps for Result Analysis

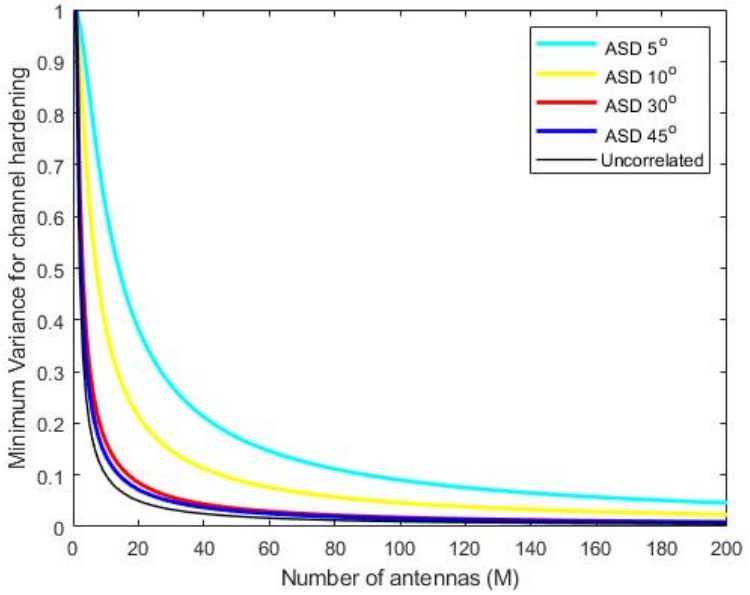

Figure 4.2: Spatial correlation effect on Channel Hardening

4.2 Impact on Channel Hardening and Favourable Propagation

The impact of spatial correlation described by nominal angle and its ASD on how many antennas are needed to approach asymptotic channel hardening and favorable propagation are explored in this section.

Channel Hardening

Recall from Section 3.5 that a channel h hardens if $\frac{\|\mathbf{h}_{jk}^{j}\|^2}{\mathbb{E}\left\{\|\mathbf{h}_{jk}^{j}\|^2\right\}} \to 1$, as $\mathrm{M_j} \to \infty$. Figure 4.2 shows the "variance" of the channel hardening as defined in equation 3.17, for different numbers of antennas The channel has hardened more, the smaller the variance. With $\varphi = 30$ and a Gaussian angular distribution with $\{\sigma_\varphi = 5°, 10°, 30°, 45°\}$ we compare uncorrelated Rayleigh fading with the local scattering model. Uncorrelated fading produces the least variation, but spatial channel correlation essentially moves the curve to the right. When σ_φ increasing (less spatially correlated), the difference from uncorrelated The amount of fading is minimal. However, there will be loss in channel hardening if the channels are strongly correlated. For example, the variance for $\sigma_\varphi = 5°$ with $M = 200$ gives the same result as uncorrelated fading with $M = 40$.

Favourable Propagation

The impact of spatial correlation on having the orthogonality of two discrete channels is shown here. Similar to channel hardening, the error variance of favorable propagation is analyzed. The ability of getting a favorable channel increases if the interfering UEs angle is different from the desired one, as described in Figure 4.3. The simulation shows that when two UEs have a similar angle towards the BS, the error variance will increase. This situation worsens when the ASD value is at its minimum. The error variance approaches

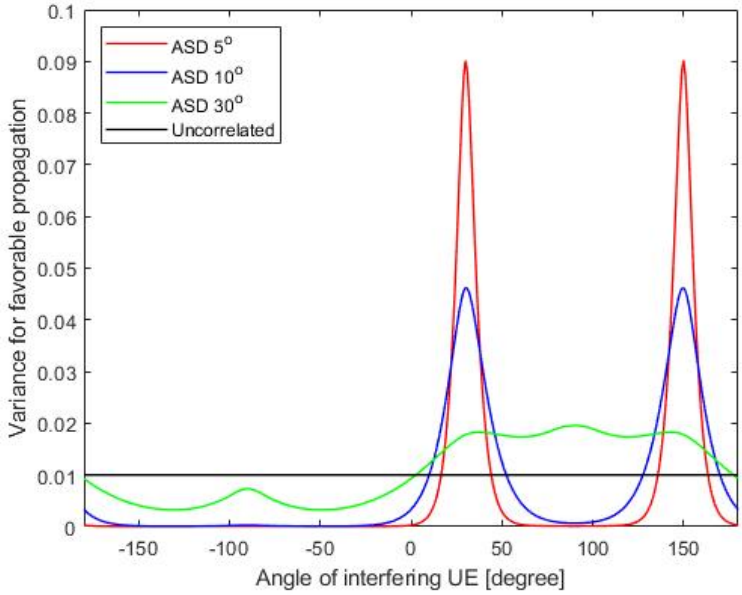

Figure 4.3: Spatial correlation effect on Favorable Propagations

the uncorrelated case as the ASD increases (take ASD = 30°). This is due to the ASD causing the deterministic angle φ to be distributed uniformly between $\pm\pi$. In that case, the distribution will tend to an uncorrelated fading scenario, but not fully uncorrelated. If the desired UE has a different Angle of Arrival (AoA) relative to interfering UEs at the BS under the minimum ASD value (take 5°) the error variance is less than the uncorrelated fading channel case.

4.3 Normalized Mean Square Error (NMSE)

In this section we analyze the simulation results of NMSE versus different measurement scenarios, recalling mathematical derivation in 3.15

Figure 4.4 SNR is generated as a function of SNR^p with various antenna values ($M = 1, 10, 100, 200$), ASD $\sigma_\varphi = 5°$, and nominal angle averaged between 0° and 360°. We can see that the NMSE is monotonically decreasing with SNR^p. At a SNR of nearly 18 dB, NMSE of approximately 10^{-2} is achieved, implying that the estimate error variance is under 1% of the channel's original variation. Interestingly, when additional antennas are added, the NMSE in Figure 4.4 decreases. This is due to spatial channel correlation, which is demonstrated by the fact that an uncorrelated spatial channel with $\mathbf{R} = \beta\mathbf{I}$ produces the NMSE $= {}^1/_{(\text{SNR}^p + 1)}$, which is independent of M. As a result of the structure in their statistics, it is easier to estimate spatially correlated channels. This also means that under spatial correlation, the predicted channel's average gain $\mathbb{E}\left\{\left\|\hat{\mathbf{h}}_{jk}^{j}\right\|^2\right\} = tr\left(\mathbf{R} - \mathbf{C}\right)$ is greater.

The impact of spatial correlation is further shown in Figure 4.5 as a function of ASD σ_φ. The analysis is based on $M = 100$ antennas and SNR $= 10$ dB. The NMSE is small when there is small value of ASD. As we discussed in favorable propagation, the scatters distributed between $\pm\pi$ exhibit approximately uncorrelated Rayleigh fading for

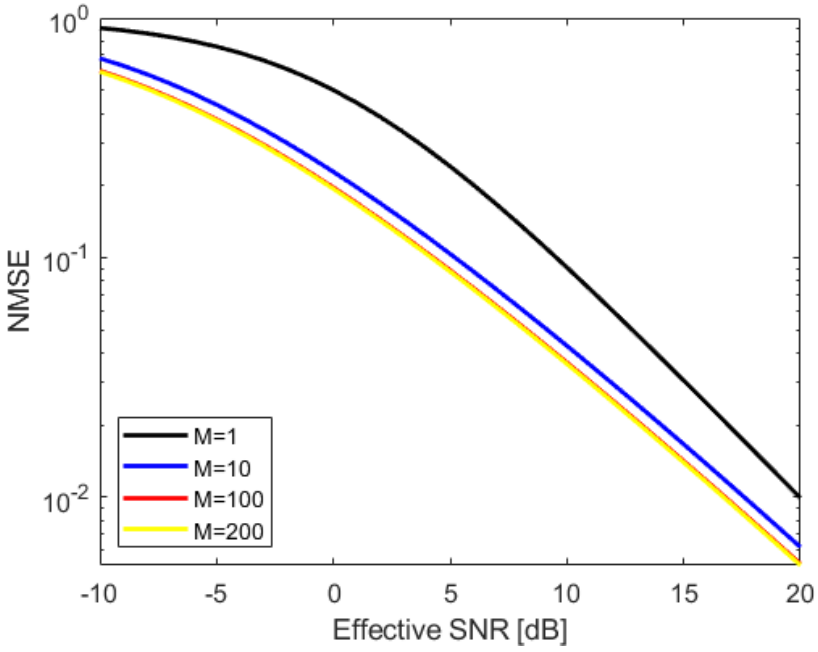

Figure 4.4: Impact of Signal Strength on NMSE

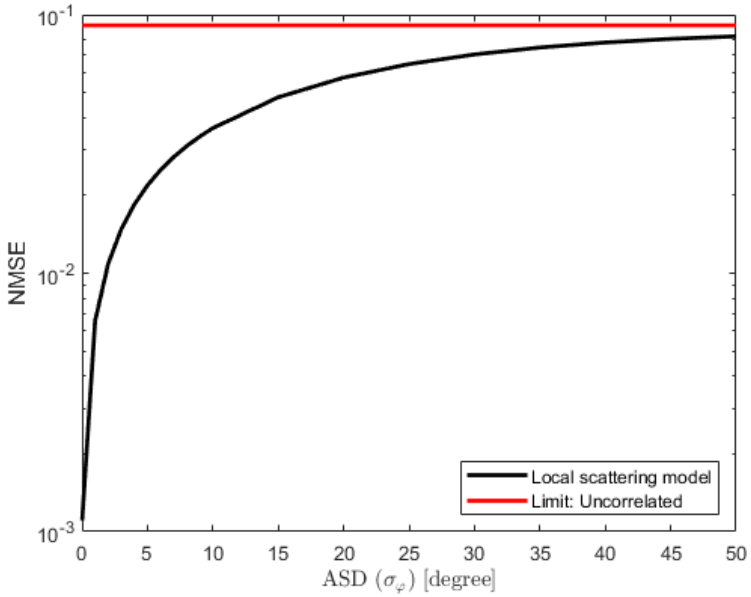

Figure 4.5: Impact of Spatial Correlation on Channel Estimation

ASD $\sigma_\varphi \to \infty$. But due to the ULA at the BS having better resolution in some directions than others, the distribution will not tend to be fully uncorrelated.

4.4 Pilot Contamination and Channel Estimation

We will now look at a situation in which two UEs use the identical pilot sequence to demonstrate the basics of pilot contamination. In its own cell, BS j estimates the channel of UE k, whereas UE i in cell l sends the same pilot. When the effective SNR from the

intended UE is 10 dB and the interfering signal is 10 dB less than the desired UE, Figure 4.6 displays the antenna-averaged correlation coefficient between the channel estimations, as specified in 3.14. The local scattering model with Gaussian angular distribution and ASD $\sigma_\varphi = 5^\circ$ is used to construct both correlation matrices, just with different nominal angles at BS j. The angle of the desired UE is fixed at 30°, whereas the angle of the interfering UE varies between -180 *and* 180 degrees. The first takeaway from Figure 4.6 is that when the BS has many antennas, the UE angles are critical. The correlation coefficient is one if the UEs have the same angle, indicating that the estimations are similar (up to a scaling factor). The correlation coefficient is virtually negligible when the UE angles are well spaced. This means that the impact of pilot contamination is determined not just by average channel gains but also by the Eigenstructure of the spatial correlation matrices. This contrasts with the single-antenna scenario (and multi-antenna case with uncorrelated fading), where the correlation coefficient is one regardless of the UEs angles. Because we are using a horizontal ULA in this simulation, the array will not be able to distinguish between signals originating from 30 and the mirror reflection angle $180^\circ - 30^\circ = 150^\circ$.

The second major effect of pilot contamination is a reduction in the accuracy of estimations. We will investigate its effect in the identical circumstances as before. Figure 4.7 inter shows the NMSE of the intended channel estimate with $M = 100$ antennas and either uncorrelated fading or the local scattering model with ASD $\sigma_\varphi = 5^\circ$. The interfering signal is either equally strong, 10 dB weaker, or 20 dB weaker than the intended UE's effective SNR. When the UEs angles are well spaced in the spatially correlated situation, the NMSE is roughly the same regardless of how strong the interfering pilot signal is. This means that when the UEs have roughly orthogonal correlation-eigenspaces, pilot contamination has little impact on estimation quality. When the UEs have similar angles, the NMSE rises, especially if the interfering UE has a strong channel to the BS. When the UEs channels show uncorrelated fading instead of spatial correlation, the NMSE are consistently greater and angle-independent. As a result, spatial channel correlation can

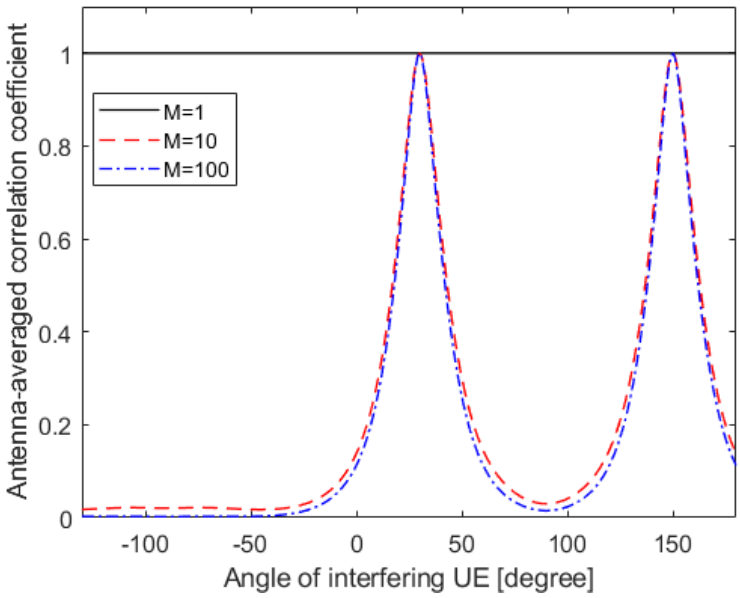

Figure 4.6: Impact of Pilot Contamination on Channel Estimation

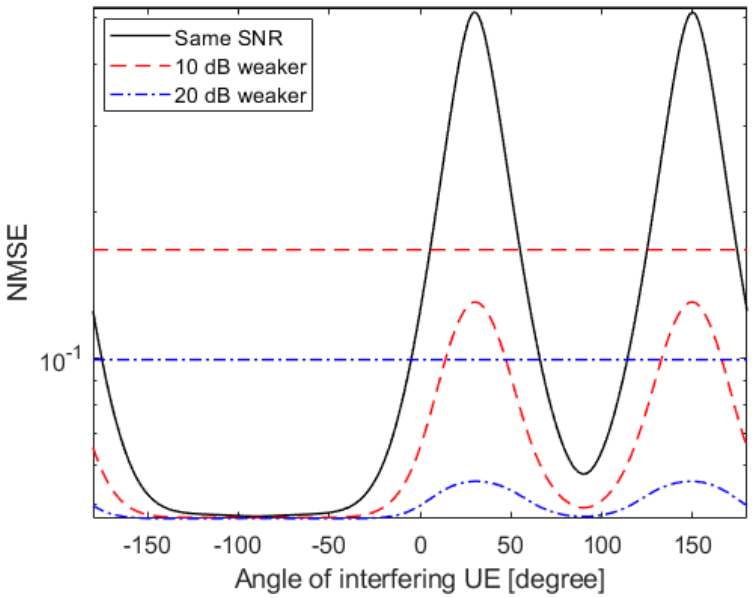

Figure 4.7: Impact of Interfering UE Signal Strength

assist in enhancing estimation quality under pilot contamination. Figure 4.7, indicates the NMSE value with a different SNR strength level of the interfering UE. As expected, the NMSE value is at its lowest when the SNR level of the interfering UE is high.

4.5 Downlink Spectral Efficiency Analysis

Each cell in the running example is placed on a square grid of 44 *cells* and covers a 0.25 km 0.25 km square. To simulate that each BS experiences equal amounts of interference from all directions, a wrap-around topology is employed. More specifically, we examine eight potential locations for the BS for each combination of UE and BS and determine which one is closest to the UE. The nominal angle between the UE and BS, as well as the large-scale fading, are calculated exclusively using this location. With a median channel gain of $\Upsilon = 148.1\ dB$ at 1 km, a pathloss exponent of $\alpha = 3.76$, and a standard deviation of the shadow fading of $sf = 10$, the large-scale fading model in equation 3.5 is applied. The NLoS macro cell 3rd Generation Partnership Project (3GPP) model for 2 GHz carriers, which is given in [71], served as the basis for these propagation parameters. The UEs are evenly and independently placed across each cell, more than 35 m away from the BS. We consider communication utilizing a 20 MHz bandwidth with a total receiver noise power of 94 dBm, which includes thermal noise and a noise figure of 7 dB in the receiver hardware. , which includes both noise and thermal noise. We assume a UL transmit power of 20 dBm per UE, with each BS allocating 20 dBm of DL transmit power per UE as necessary. With these settings, a UE's median SNR at 35 $meters$ from its serving BS is 20.6 dB, but a UE at any square cell's corner receives 5.8 dB. Because the median eliminates the effect of shadow fading, the simulations produce bigger SNR fluctuations. The size of the coherence block is subjected to an outdoor deployment scenario. Under this scenario, the value of the coherence time T_C quantified as $1ms$ and the coherence bandwidth B_C has a value of 200 KHz. Taking these values, the size of the coherence block will be 200 $samples\ \ per\ coherence\ block$. The network's

Parameter	Value
Network layout	Square
Number of cells	16
Cell area	0.25Km X 0.25Km
Number of antennas per cell	M variable
UEs per cell	K = 10
Channel gain at $1Km$	$\Upsilon = -148$ dB
UEs location	Random
ASD	5°
Path loss exponent	$\alpha = 3.76$
Shadow fading (standard deviation)	$\sigma_s f = 10$
Receiver noise power	-94 dBm
UL transmit power	20 dBm
DL transmit power	20 dBm
Samples per coherence block	$\tau_c = 200$ samples
Pilot reuse factor	$r = 1, 2, 4\ or 16$
Pilot samples	$\tau_p = rK\ samples$
DL samples	$\tau_d = \tau_c - rK$

Table 4.1: Simulation Parameters

maximum speed without the effect of a fading channel, which is $v = {}^{\lambda}/_{4T_C} = 135^{Km}/_{hr}$ is an acceptable speed. Similarly, for a given coherence bandwidth, the delay spread T_d can be calculated as $T_d = {}^{1}/_{2B_C} = 2\mu s$. Table 4.1 shows summary of all simulation parameters with their correspondent values.

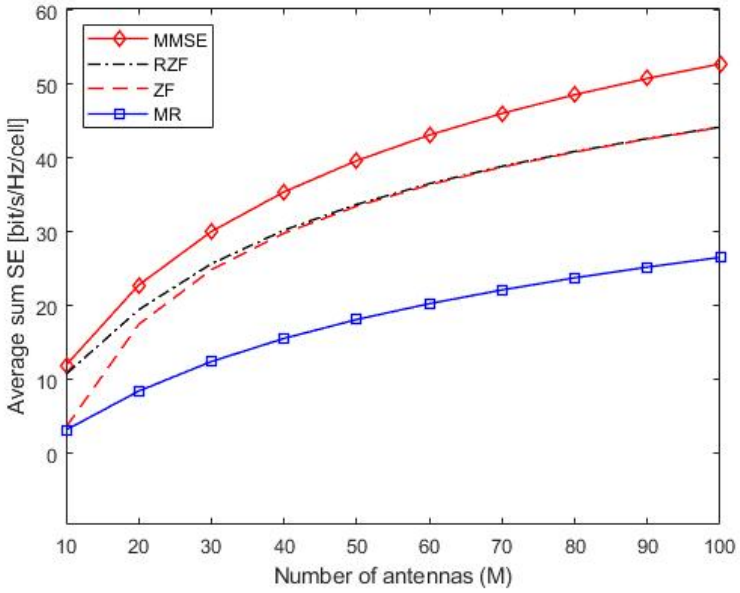

Figure 4.8: Downlink SE with pilot reuse factor r = 1

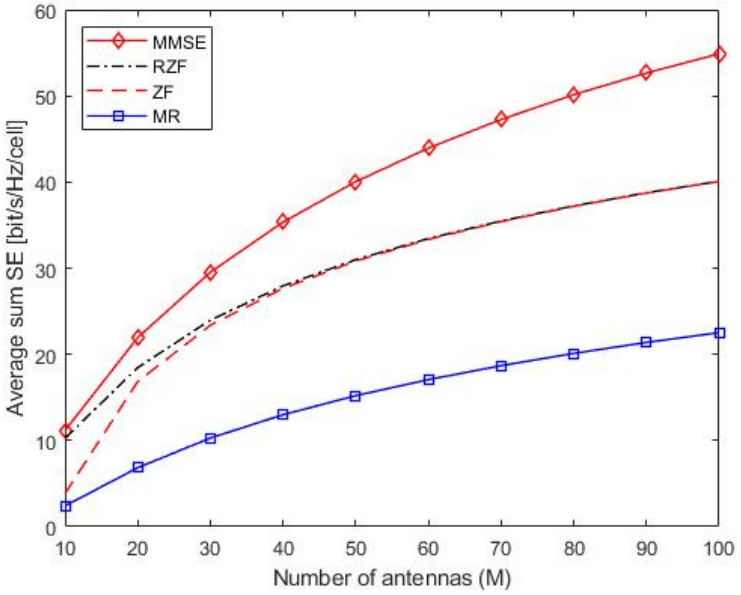

Figure 4.9: Downlink SE with pilot reuse factor r = 2

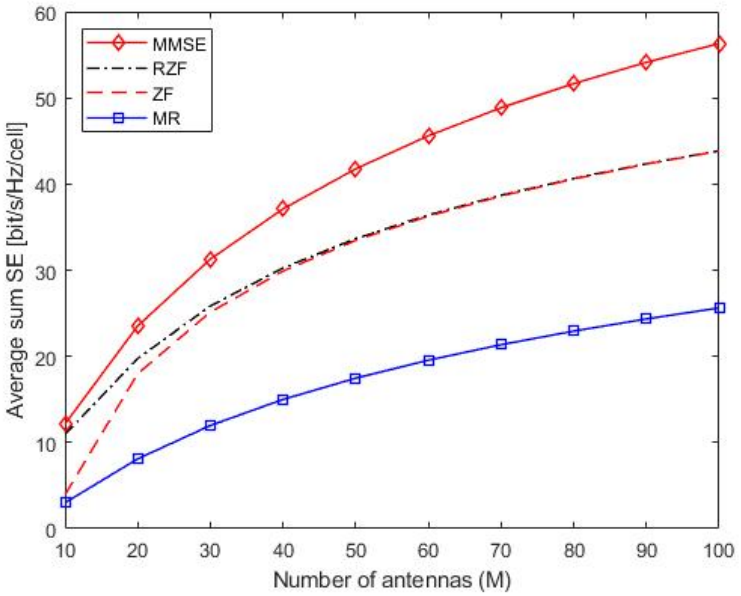

Figure 4.10: Downlink SE with pilot reuse factor r = 4

Figures 4.8 - 4.11 shows the simulation results of the SE in the DL with different pilot reuse factors. The maximum values of different precoding schemes in $[bits/s/Hz/cell]$ simulation result are also tabulated in Table 4.2. We can observe that the SE using the NMSE precoding has exhibited the largest value in the all-reuse factors. This is because the MMSE precoding is formed by considering the estimations of all UEs in the entire network. From Table 4.2 MMSE with a reuse pattern of four earns the best performance, since interference due to pilot reuse will be minimized as the reuse factor increases, as most of the interference originates from nearby cells. The second-largest value is found using the RZF precoding scheme. The RZF has a better SE when number of antennas at

Precoding Schemes	r = 1	r = 2	r = 4
MMSE	52.78	54.88	**56.3**
RZF	**44.22**	43.83	40.07
ZF	**44.21**	43.80	40.062
MRT	**26.58**	25.62	22.52

Table 4.2: Maximum Value of Precoding Schemes under Different Reuse Factor

the BS is minimum. As compared to ZF, RZF have high value when we have minimum number of antennas, due to regularization parameter dominates when there is reduction in the array gain . When the number of antennas increases (consider $M \geq 40$) ZF has the same value as RZF, because the regularized term will vanish as number of antennas at the BS increases $M \to \infty$. Since the estimate is only used to combine the intended signal coherently and not to interference suppression , the enhanced estimation quality does not offset the decreased pre-log factor, the SE of MRT decreases as r increases. The list value from all simulations goes to MRT.

For comparative purposes, Figure 4.11 is included in the simulation result of SE with a reuse factor of sixteen (that every UEs in the entire network has a unique pilot sequence). The result indicates that the SE with this reuse factor has the worst value as compared to another reuse factor. This is because generating an orthogonal pilot sequence for entire UEs in the network will result in the coherence block adding more samples to the pilot signal alone. This will reduce the samples for data transmission. In the running example, 160 samples are needed for pilot signaling (that is 80% of 200 samples).

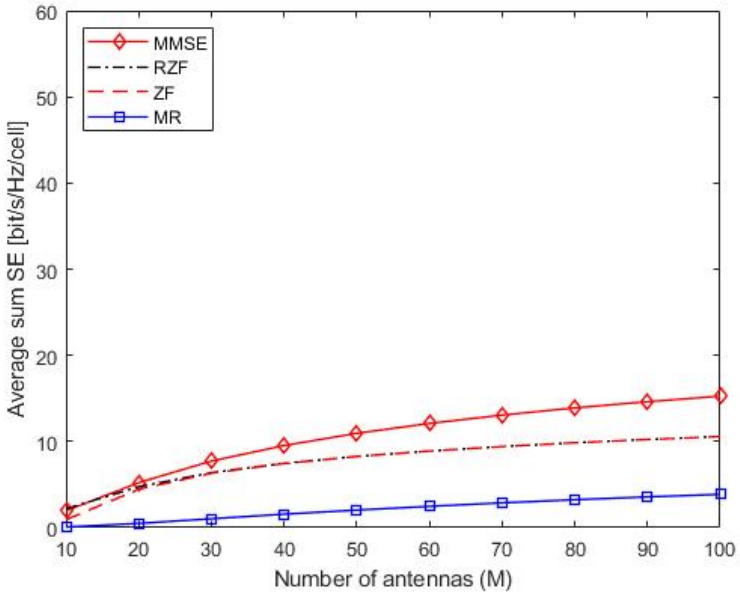

Figure 4.11: Downlink SE with pilot reuse factor r = 16

Chapter 5

Conclusion and Recommendation

5.1 Conclusion

In this thesis, we used a quantitative approach to see the impact of pilot contamination based on the distribution of UEs. The combined impact of pilot contamination and spatial correlation on channel estimation and SE is explored. The channel modeling is based on the local scattering Laplacian angle, ASD.

We observed that, the degree of channel hardening seen for a certain number of antennas is decreased by spatial channel correlation. If the UEs have distinct spatial features, spatial correlation can potentially increase the amount of favorable propagation.

Since the channel coherence blocks have a finite size, pilot sequences must be reused across cells. The inter-cell interference causes two UEs that utilize the same pilot's channel estimations to correlate, and it also increases estimation errors. When the interfering UE's channel gain is modest relative to the targeted UE's or when the correlation matrices are sufficiently dissimilar, the pilot contamination impact is minimal.

With more BS antennas, the SE increases constantly. Despite the widespread misconception that there is a basic top limit, there is no upper SE limit when utilizing MMSE in the circumstances of practical interest. This is true for MMSE channel estimation since all interference and noise are eliminated and lose their effect asymptotically. The BS is able to reject the coherent interference thanks to spatial correlation. Since only the effects of noise and non-coherent interference disappear, other techniques (like MRT and RZF) possess asymptotic upper SE bounds imposed by coherent interference from pilots.

5.2 Recommendations and Future Works

Here is a list of suggestions for prospective expansions of this thesis research's work:

- Modeling the spatial channel modeling in three dimensions 3D, the BS can trace the intended UE not only by its azimuth angle but also by vertical angle from interfering UEs. This will minimize the estimation error arises due to pilot reuse.
- It is important to research and put into practice adaptive transmit beamforming, which is essential for very large antenna arrays to have superior spectrum and energy efficiency.
- Implementing optimized pilot sequence design method will boost the SE.

References

[1] A. Osseiran, F. Boccardi, V. Braun, K. Kusume, P. Marsch, M. Maternia, O. Queseth, M. Schellmann, H. Schotten, H. Taoka, *et al.*, "Scenarios for 5g mobile and wireless communications: the vision of the metis project," *IEEE communications magazine*, vol. 52, no. 5, pp. 26–35, 2014.

[2] J. Navarro-Ortiz, P. Romero-Diaz, S. Sendra, P. Ameigeiras, J. J. Ramos-Munoz, and J. M. Lopez-Soler, "A survey on 5g usage scenarios and traffic models," *IEEE Communications Surveys & Tutorials*, vol. 22, no. 2, pp. 905–929, 2020.

[3] T. L. Marzetta, "Noncooperative cellular wireless with unlimited numbers of base station antennas," *IEEE transactions on wireless communications*, vol. 9, no. 11, pp. 3590–3600, 2010.

[4] E. Björnson, E. G. Larsson, and T. L. Marzetta, "Massive mimo: Ten myths and one critical question," *IEEE Communications Magazine*, vol. 54, no. 2, pp. 114–123, 2016.

[5] D. W. K. Ng, E. S. Lo, and R. Schober, "Energy-efficient resource allocation in ofdma systems with large numbers of base station antennas," *IEEE Transactions on Wireless Communications*, vol. 11, no. 9, pp. 3292–3304, 2012.

[6] V. W. Wong, R. Schober, D. W. K. Ng, and L.-C. Wang, *Key technologies for 5G wireless systems*. Cambridge university press, 2017.

[7] E. G. Larsson, O. Edfors, F. Tufvesson, and T. L. Marzetta, "Massive mimo for next generation wireless systems," *IEEE communications magazine*, vol. 52, no. 2, pp. 186–195, 2014.

[8] J. G. Andrews, S. Buzzi, W. Choi, S. V. Hanly, A. Lozano, A. C. Soong, and J. C. Zhang, "What will 5g be?," *IEEE Journal on selected areas in communications*, vol. 32, no. 6, pp. 1065–1082, 2014.

[9] E. G. Larsson and L. Van der Perre, "Massive mimo for 5g," 2017.

[10] J. Hoydis, S. Ten Brink, and M. Debbah, "Massive mimo in the ul/dl of cellular networks: How many antennas do we need?," *IEEE Journal on selected Areas in Communications*, vol. 31, no. 2, pp. 160–171, 2013.

[11] T. L. Marzetta and H. Q. Ngo, *Fundamentals of massive MIMO*. Cambridge University Press, 2016.

[12] L. Sanguinetti, E. Björnson, and J. Hoydis, "Toward massive mimo 2.0: Understanding spatial correlation, interference suppression, and pilot contamination," *IEEE Transactions on Communications*, vol. 68, no. 1, pp. 232–257, 2019.

[13] N. Krishnan, R. D. Yates, and N. B. Mandayam, "Uplink linear receivers for multi-cell multiuser mimo with pilot contamination: Large system analysis," *IEEE Transactions on Wireless Communications*, vol. 13, no. 8, pp. 4360–4373, 2014.

[14] K. Guo, Y. Guo, G. Ascheid, *et al.*, "Uplink power control with mmse receiver in multi-cell mu-massive-mimo systems," in *2014 IEEE International Conference on Communications (ICC)*, pp. 5184–5190, IEEE, 2014.

[15] A. B. D. H. and A. K, "Performance analysis of precoding techniques for 5g massive mimo and wireless systems," *Unpublished Masters Thesis*, 2018.

[16] V. Selvan, M. Iqbal, and H. Al-Raweshidy, "Performance analysis of linear precoding schemes for very large multi-user mimo downlink system," in *Fourth edition of the International Conference on the Innovative Computing Technology (INTECH 2014)*, pp. 219–224, IEEE, 2014.

[17] W. A. Ali, W. R. Anis, and H. A. Elshenawy, "Spectral efficiency enhancement in massive mimo system under pilot contamination," *International Journal of Communication Systems*, vol. 33, no. 8, p. e4342, 2020.

[18] H. Q. Ngo and E. G. Larsson, "No downlink pilots are needed in tdd massive mimo," *IEEE Transactions on Wireless Communications*, vol. 16, no. 5, pp. 2921–2935, 2017.

[19] X. Li, E. Björnson, E. G. Larsson, S. Zhou, and J. Wang, "Massive mimo with multi-cell mmse processing: Exploiting all pilots for interference suppression," *EURASIP Journal on Wireless Communications and Networking*, vol. 2017, no. 1, pp. 1–15, 2017.

[20] H. Q. Ngo, M. Matthaiou, and E. G. Larsson, "Performance analysis of large scale mu-mimo with optimal linear receivers," in *2012 Swedish Communication Technologies Workshop (Swe-CTW)*, pp. 59–64, IEEE, 2012.

[21] C. E. Shannon, "A mathematical theory of communication," *The Bell system technical journal*, vol. 27, no. 3, pp. 379–423, 1948.

[22] E. Björnson, J. Hoydis, and L. Sanguinetti, "Massive mimo networks: Spectral, energy, and hardware efficiency," *Foundations and Trends in Signal Processing*, vol. 11, no. 3-4, pp. 154–655, 2017.

[23] X. Shang, B. Chen, G. Kramer, and H. V. Poor, "Noisy-interference sum-rate capacity of parallel gaussian interference channels," *IEEE Transactions on Information Theory*, vol. 57, no. 1, pp. 210–226, 2010.

[24] X. Shang, G. Kramer, and B. Chen, "A new outer bound and the noisy-interference sum–rate capacity for gaussian interference channels," *IEEE Transactions on Information theory*, vol. 55, no. 2, pp. 689–699, 2009.

[25] A. S. Motahari and A. K. Khandani, "Capacity bounds for the gaussian interference channel," *IEEE Transactions on Information Theory*, vol. 55, no. 2, pp. 620–643, 2009.

[26] V. S. Annapureddy and V. V. Veeravalli, "Gaussian interference networks: Sum capacity in the low-interference regime and new outer bounds on the capacity region," *IEEE Transactions on Information Theory*, vol. 55, no. 7, pp. 3032–3050, 2009.

[27] V. S. Annapureddy and V. V. Veeravalli, "Sum capacity of mimo interference channels in the low interference regime," *IEEE Transactions on Information Theory*, vol. 57, no. 5, pp. 2565–2581, 2011.

[28] D. López-Pérez, M. Ding, H. Claussen, and A. H. Jafari, "Towards 1 gbps/ue in cellular systems: Understanding ultra-dense small cell deployments," *IEEE Communications Surveys & Tutorials*, vol. 17, no. 4, pp. 2078–2101, 2015.

[29] H. Peterson, H. Beverage, and J. Moore, "Diversity telephone receiving system of rca communications, inc.," *Proceedings of the Institute of Radio Engineers*, vol. 19, no. 4, pp. 562–584, 1931.

[30] H. T. Friis and C. B. Feldman, "A multiple unit steerable antenna for short-wave reception," *Proceedings of the Institute of Radio Engineers*, vol. 25, no. 7, pp. 841–917, 1937.

[31] E. Alexanderson, "Transoceanic radio communication," *Transactions of the American Institute of Electrical Engineers*, vol. 38, no. 2, pp. 1269–1285, 1919.

[32] B. D. Van Veen and K. M. Buckley, "Beamforming: A versatile approach to spatial filtering," *IEEE assp magazine*, vol. 5, no. 2, pp. 4–24, 1988.

[33] J. H. Winters, "Smart antennas for wireless systems," *IEEE Personal Communications*, vol. 5, no. 1, pp. 23–27, 1998.

[34] S. Anderson, B. Hagerman, H. Dam, U. Forssen, J. Karlsson, F. Kronestedt, S. Mazur, and K. J. Molnar, "Adaptive antennas for gsm and tdma systems," *IEEE Personal Communications*, vol. 6, no. 3, pp. 74–86, 1999.

[35] X. Gao, O. Edfors, F. Rusek, and F. Tufvesson, "Linear pre-coding performance in measured very-large mimo channels," in *2011 IEEE Vehicular Technology Conference (VTC Fall)*, pp. 1–5, IEEE, 2011.

[36] J. Hoydis, C. Hoek, T. Wild, and S. ten Brink, "Channel measurements for large antenna arrays," in *2012 International Symposium on Wireless Communication Systems (ISWCS)*, pp. 811–815, IEEE, 2012.

[37] M. Korb and T. G. Noll, "Ldpc decoder area, timing, and energy models for early quantitative hardware cost estimates," in *2010 International Symposium on System on Chip*, pp. 169–172, IEEE, 2010.

[38] S. C. Swales, M. A. Beach, D. J. Edwards, and J. P. McGeehan, "The performance enhancement of multibeam adaptive base-station antennas for cellular land mobile radio systems," *IEEE Transactions on Vehicular Technology*, vol. 39, no. 1, pp. 56–67, 1990.

[39] J. Winters, "Optimum combining for indoor radio systems with multiple users," *IEEE Transactions on communications*, vol. 35, no. 11, pp. 1222–1230, 1987.

[40] S. Anderson, U. Forssén, J. Karlsson, T. Witzschel, P. Fischer, and A. Krug, "Ericsson/mannesmann gsm field-trials with adaptive antennas," in *IEE Colloquium on*

Advanced TDMA Techniques and Applications (Digest No: 1996/234, pp. 6–1, IET, 1996.

[41] G. Caire and S. Shamai, "On the achievable throughput of a multiantenna gaussian broadcast channel," *IEEE Transactions on Information Theory*, vol. 49, no. 7, pp. 1691–1706, 2003.

[42] A. Goldsmith, S. A. Jafar, N. Jindal, and S. Vishwanath, "Capacity limits of mimo channels," *IEEE Journal on selected areas in Communications*, vol. 21, no. 5, pp. 684–702, 2003.

[43] F. Rashid-Farrokhi, L. Tassiulas, and K. R. Liu, "Joint optimal power control and beamforming in wireless networks using antenna arrays," *IEEE transactions on communications*, vol. 46, no. 10, pp. 1313–1324, 1998.

[44] S. Shamai and B. M. Zaidel, "Enhancing the cellular downlink capacity via co-processing at the transmitting end," in *IEEE VTS 53rd Vehicular Technology Conference, Spring 2001. Proceedings (Cat. No. 01CH37202)*, vol. 3, pp. 1745–1749, IEEE, 2001.

[45] J. H. Kotecha and A. M. Sayeed, "Transmit signal design for optimal estimation of correlated mimo channels," *IEEE Transactions on Signal Processing*, vol. 52, no. 2, pp. 546–557, 2004.

[46] Y. Liu, T. F. Wong, and W. W. Hager, "Training signal design for estimation of correlated mimo channels with colored interference," *IEEE Transactions on Signal Processing*, vol. 55, no. 4, pp. 1486–1497, 2007.

[47] G. J. Foschini and M. J. Gans, "On limits of wireless communications in a fading environment when using multiple antennas," *Wireless personal communications*, vol. 6, no. 3, pp. 311–335, 1998.

[48] P. P. Tayade and V. M. Rohokale, "Enhancement of spectral efficiency, coverage and channel capacity for wireless communication towards 5g," in *2015 International Conference on Pervasive Computing (ICPC)*, pp. 1–5, IEEE, 2015.

[49] P. Patcharamaneepakorn, S. Wu, C.-X. Wang, M. M. Alwakeel, X. Ge, M. Di Renzo, *et al.*, "Spectral, energy, and economic efficiency of 5g multicell massive mimo systems with generalized spatial modulation," *IEEE Transactions on Vehicular Technology*, vol. 65, no. 12, pp. 9715–9731, 2016.

[50] E. Larsson and E. Björnson, "Massive mimo news—commentary—mythbusting," tech. rep., Tech. Rep.[Online]. Available: http://www. massive-mimo. net.

[51] D. Tse and P. Viswanath, *Fundamentals of wireless communication*. Cambridge university press, 2005.

[52] E. Björnson and E. Jorswieck, *Optimal resource allocation in coordinated multi-cell systems*. Now Publishers Inc, 2013.

[53] E. Björnson, M. Matthaiou, and M. Debbah, "Massive mimo with non-ideal arbitrary arrays: Hardware scaling laws and circuit-aware design," *IEEE Transactions on Wireless Communications*, vol. 14, no. 8, pp. 4353–4368, 2015.

[54] A. Paulraj, A. P. Rohit, R. Nabar, and D. Gore, *Introduction to space-time wireless communications*. Cambridge university press, 2003.

[55] E. Björnson, E. G. Larsson, and M. Debbah, "Massive mimo for maximal spectral efficiency: How many users and pilots should be allocated?," *IEEE Transactions on Wireless Communications*, vol. 15, no. 2, pp. 1293–1308, 2015.

[56] S. M. Kay, *Fundamentals of statistical signal processing: estimation theory*. Prentice-Hall, Inc., 1993.

[57] G. Caire, N. Jindal, M. Kobayashi, and N. Ravindran, "Multiuser mimo achievable rates with downlink training and channel state feedback," *IEEE Transactions on Information Theory*, vol. 56, no. 6, pp. 2845–2866, 2010.

[58] M. Pinsker, V. Prelov, and E. Van der Meulen, "Information transmission over channels with additive-multiplicative noise," in *Proceedings. 1998 IEEE International Symposium on Information Theory (Cat. No. 98CH36252)*, p. 239, IEEE, 1998.

[59] T. K. Sarkar, Z. Ji, K. Kim, A. Medouri, and M. Salazar-Palma, "A survey of various propagation models for mobile communication," *IEEE Antennas and propagation Magazine*, vol. 45, no. 3, pp. 51–82, 2003.

[60] T. Trump and B. Ottersten, "Estimation of nominal direction of arrival and angular spread using an array of sensors," *Signal Processing*, vol. 50, no. 1-2, pp. 57–69, 1996.

[61] H. Yin, D. Gesbert, M. Filippou, and Y. Liu, "A coordinated approach to channel estimation in large-scale multiple-antenna systems," *IEEE Journal on selected areas in communications*, vol. 31, no. 2, pp. 264–273, 2013.

[62] F. Adachi, M. Feeney, J. Parsons, and A. Williamson, "Crosscorrelation between the envelopes of 900 mhz signals received at a mobile radio base station site," in *IEE Proceedings F-Communications, Radar and Signal Processing*, vol. 133, pp. 506–512, IET, 1986.

[63] P. Zetterberg and B. Ottersten, "The spectrum efficiency of a base station antenna array system for spatially selective transmission," *IEEE Transactions on Vehicular Technology*, vol. 44, no. 3, pp. 651–660, 1995.

[64] Z. Jiang, A. F. Molisch, G. Caire, and Z. Niu, "Achievable rates of fdd massive mimo systems with spatial channel correlation," *IEEE Transactions on Wireless Communications*, vol. 14, no. 5, pp. 2868–2882, 2015.

[65] K. I. Pedersen, P. E. Mogensen, and B. H. Fleury, "Power azimuth spectrum in outdoor environments," *Electronics Letters*, vol. 33, no. 18, pp. 1583–1584, 1997.

[66] A. Adhikary, J. Nam, J.-Y. Ahn, and G. Caire, "Joint spatial division and multiplexing—the large-scale array regime," *IEEE transactions on information theory*, vol. 59, no. 10, pp. 6441–6463, 2013.

[67] J. Salz and J. H. Winters, "Effect of fading correlation on adaptive arrays in digital mobile radio," *IEEE transactions on Vehicular Technology*, vol. 43, no. 4, pp. 1049–1057, 1994.

[68] D.-S. Shiu, G. J. Foschini, M. J. Gans, and J. M. Kahn, "Fading correlation and its effect on the capacity of multielement antenna systems," *IEEE Transactions on communications*, vol. 48, no. 3, pp. 502–513, 2000.

[69] E. A. Jorswieck and E. G. Larsson, "The miso interference channel from a game-theoretic perspective: A combination of selfishness and altruism achieves pareto optimality," in *2008 IEEE International Conference on Acoustics, Speech and Signal Processing*, pp. 5364–5367, IEEE, 2008.

[70] E. Björnson, M. Bengtsson, and B. Ottersten, "Optimal multiuser transmit beamforming: A difficult problem with a simple solution structure [lecture notes]," *IEEE Signal Processing Magazine*, vol. 31, no. 4, pp. 142–148, 2014.

[71] 3GPP, "Further advancements for e-utra physical layer aspects," *Technical Report*, 2010.